SLAC-PUB-10277
December 2003

Higgsless Electroweak Symmetry Breaking in Warped Backgrounds: Constraints and Signatures *

H. Davoudiasl[1,a], J.L. Hewett[2,b], B. Lillie[2,c], and T.G. Rizzo[2,d†]

[1] *School of Natural Sciences, Institute for Advanced Study, Princeton, NJ 08540*

[2] *Stanford Linear Accelerator Center, Stanford, CA, 94309*

Abstract

A warped 5-dimensional $SU(2)_L \times SU(2)_R \times U(1)_{B-L}$ model has been recently proposed to implement electroweak symmetry breaking through boundary conditions, without the presence of a Higgs boson. This proposal is based on the Randall-Sundrum hierarchy solution. We use precision electroweak data to constrain the general parameter space of this model. Our analysis includes independent L and R gauge couplings, radiatively induced boundary gauge kinetic terms, and all higher order corrections from the curvature of the 5-d space. We show that this setup can be brought into good agreement with the precision electroweak data for typical values of the parameters. However, this set of parameters leads to violation of unitarity in gauge boson scattering, and hence this model is excluded in its present form. Assuming that unitarity can be restored in a modified version of this scenario, we consider the collider signatures. It is found that new spin-1 states will be observed at the LHC and measurement of their properties would identify this model. However, the spin-2 graviton Kaluza-Klein resonances, which are a hallmark of the Randall-Sundrum model, are too weakly coupled to be detected.

*Work supported in part by the Department of Energy, Contract DE-AC03-76SF00515

†e-mails: [a]hooman@ias.edu, [b]hewett@slac.stanford.edu, [c]lillieb@slac.stanford.edu, and [d]rizzo@slac.stanford.edu

1 Introduction

After more than 30 years of experimental investigation, the mechanism for electroweak Symmetry Breaking (EWSB) remains unknown. The simplest picture of EWSB employs a scalar field, the Higgs, whose vacuum expectation value provides masses for the Standard Model (SM) $W^{\pm}$, Z bosons, as well as for the fermions. Experiments have yet to find this particle, even though generic expectations place it within the reach of recent searches. Direct searches [1] place the lower limit on the Higgs mass of $m_h \gtrsim 114$ TeV, whereas a global fit to the precision electroweak data set [2] places the indirect upper bound of $m_h < 219$ GeV at 95% CL.

On a more theoretical level, a weak scale Higgs scalar seems unnatural, as its mass is typically expected to receive large radiative corrections from UV physics. Thus, a hierarchy problem arises, as there seem to be much higher scales present in Nature, such as the Planck scale of gravity, $\overline{M}_{Pl} \sim 10^{18}$ GeV. This problem may be resolved by the addition of new physics at the weak scale, such as Higgs compositeness, strong dynamics (technicolor), or supersymmetry. None of these proposals have been experimentally verified, and they also suffer from various phenomenological problems.

Over the past few years, the possibility of extra spatial dimensions has been exploited to address the hierarchy conundrum. In particular, the warped 5-dimensional (5-d) Randall-Sundrum (RS) model [3], which is based on a truncated AdS_5 spacetime, offers a natural geometric setup for explaining the size of the weak scale. In this model, the weak scale is generated exponentially from the curvature of the extra dimensional space. The AdS/CFT conjecture in string theory [4] suggests that the RS model is dual to a 4-d strongly interacting field theory. The Higgs in the 5-d picture is then identified with a dual 4-d composite scalar.

It has been recently proposed [5] that one could use the boundary conditions of a 5-d flat space $\mathrm{SU}(2)_L \times \mathrm{SU}(2)_R \times \mathrm{U}(1)_{B-L}$ theory to generate masses for $W^{\pm}$ and Z bosons of the SM, in the absence of a Higgs scalar. This proposal predicted unacceptably large deviations from precision EW data and seemed to be excluded. However in Ref.[6], this Higgsless approach to EWSB was studied in the context of the RS geometry, and agreement with data was much improved. This can be understood from the fact that the model contains a custodial SU(2) symmetry which is broken only by terms of size of order the spatial variance of the bulk W and Z wavefunctions. In the warped geometry, these wavefunctions are nearly

flat over most of the bulk, as opposed to the $\mathcal{O}(1)$ spatial variance in the case of flat space.

Using the AdS/CFT correspondence [4], one may think of this proposal as a technicolor model without a Higgs scalar. This duality also addresses the improved agreement of the warped model with data, since the global $\mathrm{SU}(2)_L \times \mathrm{SU}(2)_R$ symmetry in the bulk provides the equivalent of a 4-d custodial symmetry that suppresses corrections to the EW observables. Here, we note that even though this construct is dual to some strong dynamics, the warped 5-d geometry could in principle provide a computationally controlled theory, with quantitative predictions.

In this paper, we study 5-d warped Higgsless model (WHM), employing a set of parameters that is more general than those used in the original model of Ref.[6]. In particular, we allow for independent bulk gauge couplings to the L and R gauge sectors, which is crucial in getting good agreement with the precision EW data. We also include the effects of boundary gauge kinetic terms, assuming that they are radiatively generated [7]. We do not specify a mechanism for fermion mass generation, but adopt a simple parametrization that could accommodate a large class of possible scenarios.[‡] In addition, our analysis incorporates all higher order corrections from the curvature of the 5-d space that were ignored in the initial work[6].

We will demonstrate that with typical values for the model parameters, good agreement with the precision EW data can be achieved. However, we have found that this region of parameter space leads to the violation of unitarity in $W_L W_L$ gauge boson scattering. In particular, we find that unitarity is violated at $\sqrt{s} \approx 2$ TeV, which is below the mass of the new states studied by Csaki *et al.* [5]. We find this model is thus excluded in its present form. However, assuming that unitarity can be restored by an appropriate modification of this scenario, *e.g.*, with the inclusion of additional non-Higgs states, we then consider the collider signatures which should be present in any generic WHM. In particular, we find that the gauge boson Kaluza Klein (KK) excitations of the strong and electroweak sectors are observable at the LHC. However, it is unlikely that the LHC experiments will be able to detect the spin-2 graviton KK resonances which constitute the most distinct signature of the conventional RS-based models.

In the next section, we introduce our formalism and notation. We then determine the couplings of the various KK towers to the SM fields in Section 3. Our predictions for

[‡]We note that a recent paper [8] has proposed a mechanism for generating the fermion masses geometrically by also employing boundary conditions from the WHM configuration.

the EW observables and the resulting parameter space constraints are given in Section 4. Unitarity is examined in Section 5 and the collider signatures of the model are discussed in section 6. Concluding remarks are given in Section 7.

2 Formalism and Notation

In the analysis that follows, we will, for the most part, follow the notation of Csaki *et al.*[6] with some modifications that are necessary to make contact with our previous work [9, 10]. For this reason we now review the RS metric in both notations. In the original RS scheme (employed in our earlier work), the 5-d metric is given by

$$ds^2 = g_{MN} dx^M dx^N = e^{-2\sigma} \eta_{\mu\nu} dx^\mu dx^\nu - dy^2 \,, \tag{1}$$

with uppercase Roman indices extending over 5-dimensional space-time and Greek indices corresponding to 4-d. Here, $\sigma = k|y| = kr_c|\phi|$, with r_c being the compactification radius, k is the curvature scale associated with the 5-d space, and $-\pi \leq \phi \leq \pi$ with ϕ parameterizing the 5th coordinate. For numerical purposes we will take $kr_c = 11.27$ throughout our analysis. The geometrical setup contains 2 branes, one residing at $\phi = 0$ (known as the Planck brane) and one at $\phi = \pi$ (the TeV brane), *i.e.*, the branes are located at the boundaries of the 5-dimensional Anti-de Sitter space. We define the quantity $\Lambda_\pi \equiv \overline{M}_{Pl} e^{-\pi k r_c}$, which represents the scale of physical processes on the TeV brane. In the scheme used in Ref. [6], this metric is rewritten as

$$ds^2 = \left(\frac{R}{z}\right)^2 (\eta_{\mu\nu} dx^\mu dx^\nu - dz^2) \,, \tag{2}$$

with $R \leq z \leq R'$. Here, we see that the relationships $k = R^{-1}$, $R' = Re^{\pi k r_c}$, and $z = e^{ky}/k$ converts one form of the metric to the other. In this convention, the Planck (TeV) brane resides at $z = R\,(R')$. It is important to note that the range $R \leq z \leq R'$ maps onto only *half* of the $-\pi \leq \phi \leq \pi$ interval. When employing the Csaki *et al.* notation in what follows, we will normalize our wavefunctions over twice the $R \leq z \leq R'$ interval for consistency with our earlier work.

In the WHM, the gauge theory in the bulk is $\mathrm{SU}(3)_C \times \mathrm{SU}(2)_L \times \mathrm{SU}(2)_R \times \mathrm{U}(1)_{B-L}$ for which the bulk action is given by

$$S = \int d^4x dy \, \sqrt{-g} \sum_i \frac{-1}{4 g_{5i}^2} F^i_{AB} F_i^{AB} \,, \tag{3}$$

where we have suppressed the group indices, $-g \equiv det(g_{MN})$, the sum extends over the four gauge groups, and g_{5i} are the appropriate 5-d coupling constants. Note that for generality, we allow for the possibility of $g_{5L} \neq g_{5R}$ in our analysis below. The boundary conditions are chosen such that the gauge symmetry breaking chain $\mathrm{SU}(2)_R \times \mathrm{U}(1)_{B-L} \to \mathrm{U}(1)_Y$ occurs at the Planck scale and subsequently the gauge symmetry breaking $\mathrm{SU}(2)_L \times \mathrm{U}(1)_Y \to \mathrm{U}(1)_{QED}$ takes place at the TeV scale. This hierarchical two-step breaking scheme is analogous to that of the usual breaking pattern of the conventional Left-Right Symmetric Model [11]. After the gauge symmetry is broken at the Planck scale, a global $\mathrm{SU}(2)_R \times \mathrm{SU}(2)_L$ symmetry remains in the brane picture. This global symmetry is broken on the TeV brane to a diagonal group, $\mathrm{SU}(2)_D$, which corresponds to the SU(2) custodial symmetry present in the SM. It is the presence of this custodial symmetry which essentially preserves the tree-level value of unity for the ρ parameter in this model. Of the 7 generators present in the high-scale electroweak sector, 3 are broken near $\overline{M}_{Pl}$, 3 are broken near the TeV scale, leaving one generator for $\mathrm{U}(1)_{QED}$ as in the SM. $\mathrm{SU}(3)_C$, of course, remains unbroken and is simply the 5-d analog of QCD.

In addition to the bulk action above, significant boundary (brane) terms can exist in this scenario [7] which can be generated via quantum contributions [12]. The only sizable effects arise at $y = 0$, *i.e.*, on the Planck brane, due to the renormalization group evolution (RGE) between the physical scales associated with the two branes, $\sim k$ and $\sim k e^{-\pi k r_c}$. Since the gauge group below the scale k is simply $\mathrm{SU}(3)_C \times \mathrm{SU}(2)_L \times \mathrm{U}(1)_Y$, only these gauge fields will have brane localized kinetic terms, which we may write as

$$S_{brane} = \int d^4x dy \, \sqrt{-g} \, \delta(y) \left\{ -\frac{1}{4\tilde{g}_L^2} F_L^{\mu\nu} F_{\mu\nu}^L - \frac{1}{4\tilde{g}_Y^2} F_Y^{\mu\nu} F_{\mu\nu}^Y - \frac{1}{4\tilde{g}_s^2} F_C^{\mu\nu} F_{\mu\nu}^C \right\} , \tag{4}$$

where

$$\frac{1}{\tilde{g}_i^2} = \frac{\beta_i}{8\pi^2} \ln\left(\frac{k}{k e^{-\pi k r_c}}\right) = \frac{\beta_i}{8\pi^2} \pi k r_c \, , \tag{5}$$

for $i = L \, , Y \, , s$ and β_i being the appropriate beta function. If only SM fields are present in the model, then $(\beta_L \, , \beta_Y \, , \beta_s) = (-10/3 \, , 20/3 \, , -7)$; we will assume these values in our numerical analysis. Note that due to the large logarithms, these coefficients can be significant, of $\mathcal{O}(1)$ or larger, and will lead to important effects as will be seen below.

In our earlier analysis [10], we introduced the notation

$$\frac{g_{5i}^2}{\tilde{g}_i^2} \equiv r_c c_i \equiv \frac{2\delta_i}{k}\,, \qquad\qquad (i = L\,, Y\,, s) \tag{6}$$

which is useful for quantifying the size of the brane kinetic terms. Given the above relations for $1/\tilde{g}_i^2$, and the assumption that only SM fields contribute to the beta functions, one can show that δ_Y is not an independent parameter, but is directly calculable. (We will return to the case of 5-d QCD later.) From Eq. (5) we have

$$\frac{1}{\tilde{g}_Y^2} = -2\frac{1}{\tilde{g}_L^2}\,, \tag{7}$$

where the factor of -2 arises from the ratio β_Y/β_L. This leads to

$$\frac{g_{5Y}^2}{\tilde{g}_Y^2} = -2\frac{g_{5Y}^2}{\tilde{g}_L^2}\,. \tag{8}$$

Since $\mathrm{SU}(2)_R\times\ \mathrm{U}(1)_{B-L} \to \mathrm{U}(1)_Y$, we have the relations

$$\frac{1}{g_{5Y}^2} = \frac{1}{g_{5R}^2} + \frac{1}{g_{5B}^2}\,, \tag{9}$$

which we can write as

$$\frac{g_{5L}^2}{g_{5Y}^2} = \frac{1}{\kappa^2} + \frac{1}{\lambda^2}\,, \tag{10}$$

by introducing the notation

$$\kappa \equiv \frac{g_{5R}}{g_{5L}}\,, \qquad\qquad \lambda \equiv \frac{g_{5B}}{g_{5L}}\,. \tag{11}$$

Solving the above for g_{5Y}^2, we obtain

$$\frac{g_{5Y}^2}{\tilde{g}_Y^2} = -2\frac{\lambda^2\kappa^2}{\lambda^2+\kappa^2}\frac{g_{5L}^2}{\tilde{g}_L^2}\,, \tag{12}$$

which yields

$$\delta_Y = -2\frac{\lambda^2\kappa^2}{\lambda^2+\kappa^2}\delta_L\,. \tag{13}$$

As we will see below, the value of λ will be determined by the $M_{W,Z}$ mass relationship while κ will remain a free parameter confined to a constrained region.

The following set of boundary conditions generate the symmetry breaking pattern discussed above (note that we suppress the Minkowski indices):

On the TeV brane at $z = R'$ $(y = \pi r_c)$ one has

$$\begin{aligned} \partial_z(g_{5R}A_L^a + g_{5L}A_R^a) &= 0\,; \qquad \partial_z A_C^a = 0\,; \\ g_{5L}A_L^a - g_{5R}A_R^a &= 0\,; \qquad \partial_z B = 0\,; \\ g_{5L}A_5^{La} + g_{5R}A_5^{Ra} &= 0\,; \qquad B_5 = 0\,; \\ \partial_z(g_{5R}A_5^{La} - g_{5L}A_5^{Ra}) &= 0\,, \end{aligned} \tag{14}$$

with $A_{L(R)}^a$ or A_C^a being one of the $\mathrm{SU}(2)_{L(R)}$ or $\mathrm{SU}(3)_C$ fields with gauge index a, and B being the corresponding $\mathrm{U}(1)_{B-L}$ field.

On the Planck brane at $z = R$ $(y = 0)$ the boundary conditions are

$$\begin{aligned} \partial_z A_L^a &= -\delta_L x_n^2 k\epsilon^2 A_L^a\,; \qquad \partial_z A_C^a = -\delta_s x_n^2 k\epsilon^2 A_C^a\,; \\ A_R^{1,2} &= 0\,; \qquad g_{5B}B - g_{5R}A_R^3 = 0\,; \\ \partial_z[g_{5B}A_R^3 &+ g_{5R}B] = -\delta_Y x_n^2 k\epsilon^2[g_{5B}A_R^3 + g_{5R}B]\,; \\ A_5^{La} &= 0\,; \qquad A_5^{Ra} = 0\,; \qquad B_5 = 0\,, \end{aligned} \tag{15}$$

where $\epsilon = e^{-\pi k r_c}$, and $m_n = x_n k\epsilon$ is the mass of the n^{th} gauge KK state. For the remainder of this paper, we will work in the unitary gauge, where the fifth components of the gauge fields are zero.

Recalling the breaking pattern for $\mathrm{SU}(2)_R\times\ \mathrm{U}(1)_{B-L} \to \mathrm{U}(1)_Y$, we introduce the fields

$$\begin{aligned} Y &= \frac{g_{5R}B + g_{5B}A_R^3}{\sqrt{g_{5R}^2 + g_{5B}^2}}\,, \\ \zeta &= \frac{g_{5B}B - g_{5R}A_R^3}{\sqrt{g_{5R}^2 + g_{5B}^2}}\,, \end{aligned} \tag{16}$$

and identify Y with the usual hypercharge field. In that case, the boundary condition on the third line in Eq. (15) can be written more simply as

$$\partial_z Y = -\delta_Y x_n^2 k\epsilon^2 Y\,. \tag{17}$$

The KK decomposition we use is essentially that of Csaki *et al.*, but allowing for $g_{5L} \neq g_{5R}$ and is expanded to include the $\mathrm{SU}(3)_C$ group:

$$\begin{aligned}
B(x,z) &= \alpha_B \gamma(x) + \sum \chi_k^B(z) Z^{(k)}(x)\,, \\
A_L^3(x,z) &= \alpha_L \gamma(x) + \sum \chi_k^{L^3}(z) Z^{(k)}(x)\,, \\
A_R^3(x,z) &= \alpha_R \gamma(x) + \sum \chi_k^{R^3}(z) Z^{(k)}(x)\,, \\
A_L^\pm(x,z) &= \sum \chi_k^{L^\pm}(z) W^{(k)\pm}(x)\,, \\
A_R^\pm(x,z) &= \sum \chi_k^{R^\pm}(z) W^{(k)\pm}(x)\,, \\
A_C(x,z) &= \alpha_g g(x) + \sum \chi_k^g(z) g^{(k)}(x)\,,
\end{aligned} \tag{18}$$

where we have again suppressed the Lorentz indices and the sum extends over the KK tower states, $k = 1...\infty$. Here, $\gamma(g)$ is the massless photon(gluon) field and $\alpha_{B,L,R,g}$ are numerical constants which are determined from the boundary conditions. Note that since the photon and gluon zero-mode states are massless, their wavefunctions are z-independent, *i.e.*, they are 'flat' in z. The wavefunctions $\chi_k^A(z)$ take the form

$$\chi_k^A(z) = z(a_A^k J_1(m_k z) + b_A^k Y_1(m_k z))\,, \tag{19}$$

with $J_1\,, Y_1$ being first-order Bessel functions with the coefficients $a_A^k\,, b_A^k$ and the KK masses m_k to be determined by the boundary conditions as we now discuss.

Let us first consider the case of the charged gauge boson sector. We first introduce the notation,

$$\begin{aligned}
R_i &\equiv Y_i(x_n^W \epsilon)/J_i(x_n^W \epsilon)\,, \\
\tilde{R}_i &\equiv Y_i(x_n^W)/J_i(x_n^W)\,,
\end{aligned} \tag{20}$$

where $x_n^W k\epsilon$ are the masses of the $W^\pm$ KK tower states. Expressions for the coefficients $b_{L,R}^\pm\,, a_R^\pm$ in terms of $a_L^\pm$ can easily be obtained via the boundary conditions; we find (dropping

the KK index for convenience)

$$\begin{aligned} b_L^{\pm} &= -\frac{a_L^{\pm}}{R_0} X_L \,, \\ b_R^{\pm} &= -\frac{a_R^{\pm}}{R_1} \,, \\ a_R^{\pm} &= -\kappa \frac{(1 - X_L \tilde{R}_0/R_0)}{(1 - \tilde{R}_0/R_1)} a_L^{\pm} \,, \end{aligned} \tag{21}$$

where $a_L^{\pm}$ will be determined by the wavefunction normalization and

$$X_L \equiv \frac{1 + \delta_L x_n^W \epsilon R_W}{1 + \delta_L x_n^W \epsilon R_1 R_W / R_0} \,, \tag{22}$$

with $R_W \equiv J_1(x_n^W \epsilon)/J_0(x_n^W \epsilon)$. The masses of the KK states can then be determined and are explicitly given by the root equation

$$(R_1 - \tilde{R}_0)(R_0 - X_L \tilde{R}_1) + \kappa^2 (R_1 - \tilde{R}_1)(R_0 - X_L \tilde{R}_0) = 0 \,. \tag{23}$$

Note that for $g_{5L} = g_{5R}$, *i.e.*, $\kappa = 1$, and in the absence of boundary terms ($\delta_L = 0$, $X_L = 1$), this expression reduces to that obtained by Csaki *et al.* [6]. We will return to a study of the roots and corresponding gauge KK masses in the next section.

We now turn to the neutral electroweak sector and first consider the massive tower states. The boundary conditions yield (where $R_i \,, \tilde{R}_i$ are defined as above with $W \to Z$)

$$\begin{aligned} b_L &= -\frac{a_L X_L}{R_0} \,, \\ b_R &= -a_L \frac{(1 - X_L \tilde{R}_1/R_0) + \kappa^2 (1 - X_L \tilde{R}_0/R_0)}{\kappa(\tilde{R}_0 - \tilde{R}_1)} \,, \\ a_R &= -\kappa a_L (1 - X_L \tilde{R}_0/R_0) - b_R \tilde{R}_0 \,, \\ b_B &= -\frac{a_B}{\tilde{R}_0} \,, \\ a_B &= -\frac{\lambda a_L (X_Y a_R/a_L + R_0 b_R/a_L)}{\kappa (X_Y - R_0/\tilde{R}_0)} \,, \end{aligned} \tag{24}$$

where now a_L is determined via normalization and we have defined

$$X_{L,Y} \equiv \frac{1+\delta_{L,Y} x_n^Z \epsilon R_Z}{1+\delta_{L,Y} x_n^Z \epsilon R_Z R_1/R_0}\,, \tag{25}$$

with $R_Z \equiv J_1(x_n^Z\epsilon)/J_0(x_n^Z\epsilon)$. The root equation for the neutral KK tower masses is then,

$$\begin{aligned}
& -\lambda^2(\tilde{R}_0 - R_1)\Big\{\kappa^2 X_Y(\tilde{R}_0-\tilde{R}_1)(R_0 - X_L - \tilde{R}_0) + (R_0 - X_L\tilde{R}_1)(R_0 - X_Y\tilde{R}_0) \\
+ \quad & \kappa^2(R_0 - X_L\tilde{R}_0)(R_0 - X_Y\tilde{R}_0)\Big\} \\
+ \quad & \kappa^2(R_0 - X_Y\tilde{R}_0)\Big\{\kappa^2(\tilde{R}_0-\tilde{R}_1)(R_0 - X_L\tilde{R}_0) + (R_1 - \tilde{R}_0)(R_0 - X_L\tilde{R}_1) \\
+ \quad & \kappa^2(R_0 - X_L\tilde{R}_0)(R_1 - \tilde{R}_0)\Big\} = 0\,.
\end{aligned} \tag{26}$$

Note that unlike the case where brane terms are neglected, this equation does not factorize into a pair of KK towers associated with the γ and Z. In fact, as we will see below, the γ and Z tower states are highly mixed and do not simply appear to be more massive copies of the SM photon and Z boson.

Turning to the case of the zero-mode photon, the fact that its wavefunction is constant in z trivializes all but two of the boundary conditions from which the coefficients in Eq. (18) may be obtained:

$$\alpha_R = \alpha_L/\kappa\,, \qquad\qquad \alpha_B = \alpha_L/\lambda\,, \tag{27}$$

with α_L to be determined via normalization of the massless photon field.

For the remaining case of $\mathrm{SU}(3)_C$, we see that α_g is determined via the normalization of the massless gluon field and the two boundary conditions lead to the single relation

$$b_s = -\frac{a_s X_s}{R_0}\,, \tag{28}$$

where X_s is defined from Eq. (22) with $x_n^W \to x_n^g$, $\delta_L \to \delta_s$. The mass spectrum of the gluon excitations are then given by the simple relation

$$R_0 - X_s\tilde{R}_0 = 0\,. \tag{29}$$

As before, a_s will be determined via the normalization conditions in the next section.

3 Determination of the KK Mass Spectrum and Couplings

In this section, we solve the various root equations to determine the mass spectrum and couplings of the KK sector. A priori, it would seem that the parameters $\kappa\,, \lambda$, and δ_L are completely arbitrary, but as we will see, some of them are determined by data. We first consider the $W^\pm$ KK tower. In this case, the root equation depends on κ and δ_L, and although $1/\tilde{g}_L^2$ is known, the ratio $g_{5L}^2/\tilde{g}_L^2$, which gives δ_L, is not. However, δ_L is not arbitrary and can be determined from the measured value of the Fermi constant in a self-consistent manner as follows. Our approach is: (i) we choose a value of κ and an input value of $\delta_L(=\delta_L^{in})$ and then calculate the roots x_n^W using Eq. (22). Since $m_{W_1} = M_W = x_1^W k\epsilon$ is identified with the physical $W^\pm$ state observed in experiment and is thus known, this fixes $k\epsilon$ so that the masses of all the KK excitations m_{W_n} can be determined. (ii) Now that the values of the x_n^W are known, the coefficients $a_R^\pm\,, b_{L,R}^\pm$ of the wavefunctions are also calculable; this allows us to determine the couplings of the KK states to the SM fermions. These are of the form

$$g_{W_n}^2 = N_n \frac{g_{5L}^2}{2\pi r_c}\,, \tag{30}$$

where the coefficients N_n are computed below. (iii) We observe that the above equation can be rewritten to give g_{5L}^2 provided that $g_{W_1}^2$, which corresponds to the usual W boson coupling, is known. We find

$$g_{5L}^2 = 2\pi r_c g_{W_1}^2/N_1\,, \tag{31}$$

so that

$$\delta_L^{out} = \pi k r_c \frac{g_{W_1}^2}{N_1 \tilde{g}_L^2}\,. \tag{32}$$

(iv) Next we must examine whether $\delta_L^{out} = \delta_L^{in}$ as a test of consistency. We recall from μ-decay that at tree-level,

$$\frac{8G_F}{\sqrt{2}} = \sum_{n=1}^{\infty} \frac{g_{W_n}^2}{m_{W_n}^2} = \frac{g_{W_1}^2}{M_W^2} \sum_{n=1}^{\infty} \frac{N_n}{N_1 (x_n^W/x_1^W)^2}\,, \tag{33}$$

with all the quantities in this equation being known except $g^2_{W_1}$. Hence solving for $g^2_{W_1}$ and inserting this result into the previous equation, we obtain a calculable expression for δ_L^{out},

$$\delta_L^{out} = \frac{\pi k r_c}{N_1 \tilde{g}_L^2} \frac{8 G_F M_W^2}{\sqrt{2}} \left[\sum_{n=1}^{\infty} \frac{N_n}{N_1 (x_n/x_1)^2} \right]^{-1} . \tag{34}$$

If $\delta_L^{out} \neq \delta_L^{in}$ for a fixed value of κ, we perform another search until convergence is obtained. When we have found a consistent solution (*i.e.*, $\delta_L^{in} = \delta_L^{out}$), $g^2_{W_n}$ and g^2_{5L} are determined absolutely as a function of κ. We would expect δ_L to only weakly depend on κ since this dependence vanishes at zeroth-order in $1/\pi k r_c \simeq 1/35$. Here, we emphasize the importance of the μ-decay constraint in obtaining this result, as G_F determines the absolute strength of the coupling g_{W_1}, thus providing a reference to which all others can be scaled. Fig. 1 displays the value of δ_L^{out} versus δ_L^{in} for $\kappa = 3$, for demonstration, and we see that a unique solution is obtained only when $\delta_L \simeq -7.8$; we find similar results for other values of κ near unity.

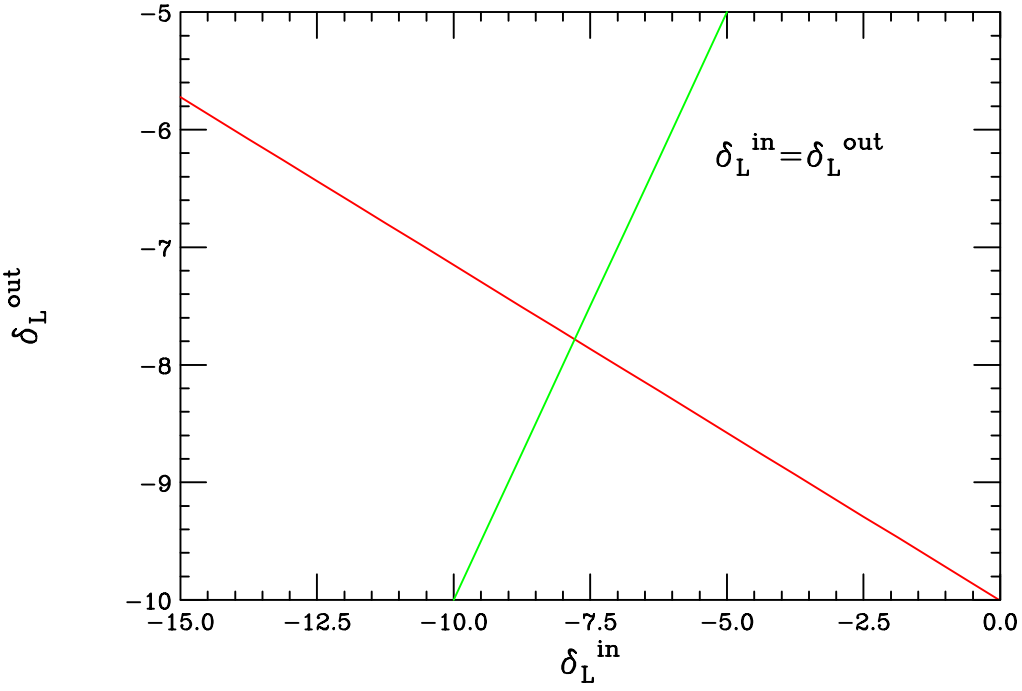

Figure 1: The value of $\delta_L (= \delta_L^{out})$ calculated via the procedure described in the text as a function of the input value (red curve). The curve corresponding to $\delta_L^{in} = \delta_L^{out}$ is also shown (green curve); the solution lies at the intersection of the two curves. Here, $\kappa = 3$ is assumed.

The parameter κ is bounded from below as can be seen from Eqs. (10) and (11) of

Ref. [7] which apply at lowest order in $1/\pi k r_c$,

$$c_w^{-2} = \frac{M_Z^2}{M_W^2} = \frac{\kappa^2\lambda^2(1+D_L) + (\kappa^2+\lambda^2)(1+D_Y)}{(\kappa^2+\lambda^2)(1+D_Y)}\,, \tag{35}$$

where $D_{L,Y} = \delta_{L,Y}/\pi k r_c$, and $c_w = \cos\theta_w$ where θ_w is the weak mixing angle. Solving for λ^2, using $D_Y = -2D_L\kappa^2\lambda^2/(\kappa^2+\lambda^2)$, and demanding that $\lambda^2 > 0$, we obtain the bound

$$\kappa^2 > \frac{c_w^{-2}-1}{1+D_L(2c_w^{-2}-1)}\,. \tag{36}$$

With $\delta_L \simeq -7.8$ and $c_w^2 \simeq 0.78$, this implies the constraint

$$\kappa \gtrsim 0.66\,. \tag{37}$$

Although there will be corrections to this result from terms of order $1/\pi k r_c$, we expect these to be no more than a few percent. To be concrete, we will assume that $\kappa \geq 0.75$ in our analysis.

It is also possible to obtain an approximate upper bound on κ based on perturbativity arguments, as the typical 4-d couplings $g_{4R}^2 \equiv g_{5R}^2/2\pi r_c$ cannot become too strong. A short analysis leads to the constraint that $\kappa \lesssim 4$. To be specific, we will thus limit ourselves to the range $0.75 \leq \kappa \leq 4$ in our study. This agrees with our expectations that on general grounds, the values of g_{5R} and g_{5L} should not be too different, implying that $\kappa \sim 1$.

Next, in order to define the KK couplings to SM fields, we need to discuss the localization of the SM fermions. (Note that we define the strength of the 'weak coupling' via the interaction of the SM $W^\pm$ boson and fermions.) In the original analysis of the WHM [5, 7], the SM fermions were all localized on the Planck brane; for further model-building purposes this need not be so [8]. However, it is well-known that if the fermions are localized close to the Planck brane their gauge couplings can be well approximated by the purely Planck brane values [13, 14]. We have checked that the gauge field wavefunctions are reasonably flat for fermions localized with $\nu \lesssim -0.6$, where the quantity ν is as defined in Ref. [13]. For simplicity, we thus make this assumption below. Under this assumption, the covariant derivative acting on these fields is given by

$$D^\mu = \partial^\mu + ig_{5L}T_L A_L^\mu + ig_{5R}T_R A_R^\mu + ig_{5B}\frac{B-L}{2}B^\mu + ig_{5s}T_s A_C^\mu\,. \tag{38}$$

In this case, following Csaki *et al.* [6] and Nomura [7], the couplings of the W_n KK states to the SM fermions are given by

$$g_{W_n}^2 = \Omega^2 \frac{g_{5L}^2 |\chi_n^{L^\pm}(R)|^2}{N_{W_n}}\,, \tag{39}$$

with

$$N_{W_n} = \int_R^{R'} dz\, \frac{R}{z} \left\{ |\chi_n^{L^\pm}(z)|^2 [2 + c_L r_c \delta(z-R)] + 2|\chi_n^{R^\pm}(z)|^2 \right\}\,, \tag{40}$$

where the relative factors of 2 arise from the interval extension discussed in the previous section. The coefficient Ω is determined numerically via the self-consistency procedure described above, which demands that for $n = 1$ (*i.e.*. the SM W boson), we recover the usual SM coupling $g_{W_1}^2 = g_{SM}^2$. Thus, the W boson coupling automatically retains its known value by construction when we identify $W_1^\pm \equiv W_{SM}^\pm$ as the experimentally observed state (and correspondingly $m_{W_1} = M_W$ through the use of G_F). Using M_W and g_{SM}^2 from experiment, we thus can determine the masses and couplings of all the higher KK modes. Here, we assume the LEPEWWG [2] central values of the SM gauge boson masses, $M_W = 80.426\,\mathrm{GeV}$ and $M_Z = 91.1875\,\mathrm{GeV}$ in our analysis.

Figure 2 displays the masses of the first few W KK excitations as a function of κ. We see that the masses grow reasonably rapidly as κ increases and can be quite heavy. For example, for $\kappa = 3$, the first $W^\pm$ excitation above the SM-like W boson, $W_2^\pm$, has a mass of $\simeq 2.32$ TeV. The masses of the higher KK states are approximately given by the root relation $x_n^W = x_2^W + (n-2)\pi$. The coupling strength of the gauge KK excitations are small relative to those for the $W^\pm$ and decrease rapidly as the KK mode number increases. *E.g.*, the first $W^\pm$ KK excitation has a fermionic coupling of only $g_{W_2}^2 \simeq 0.0431 g_{SM}^2$. As we will see below, this will have important implications in the consideration of unitarity violation in $W_L W_L$ scattering.

We now turn to the neutral KK states and first discuss their mass spectrum. We will refer to these states as Z_n, but they are KK excitations of both the γ and Z and are mixtures thereof. In our analysis, we will force the W and Z bosons to have the correct masses, *i.e.*, those given by experiment, and will also make use of the on-shell definition of the weak mixing angle.

$$\cos^2\theta_w^{os} \equiv \frac{M_W^2}{M_Z^2}\,. \tag{41}$$

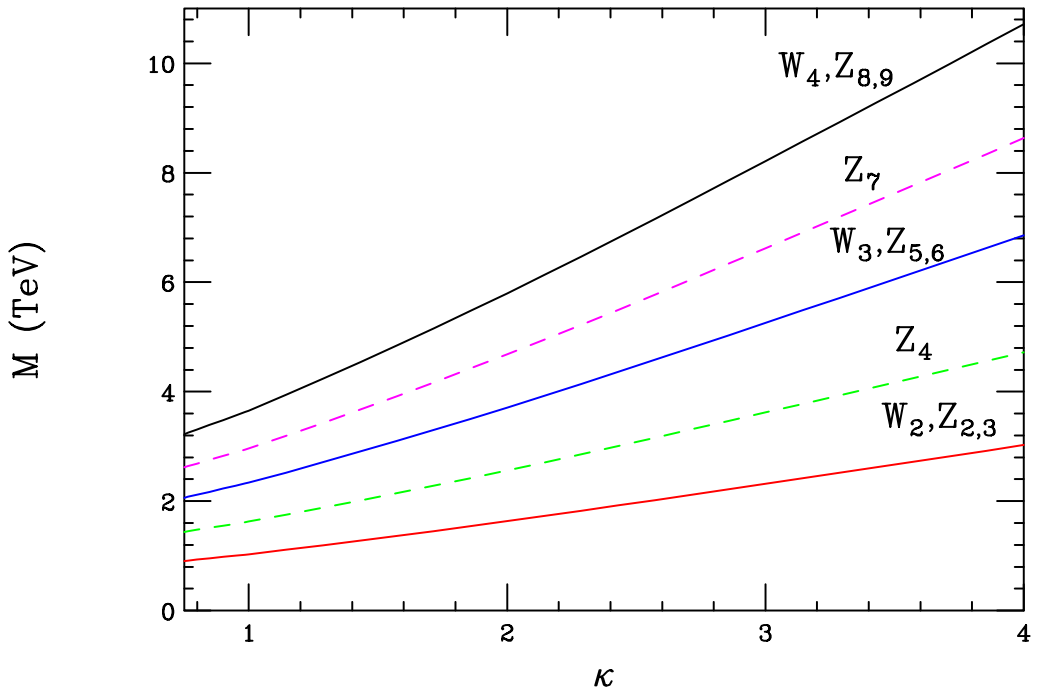

Figure 2: Masses of the electroweak gauge KK excitations as a function of κ. The solid curves correspond to the $W^{\pm}$ states, while the Z KK excitations correspond to both the solid and dashed curves as labeled. In the latter case, the solid curves correspond to the almost doubly degenerate states.

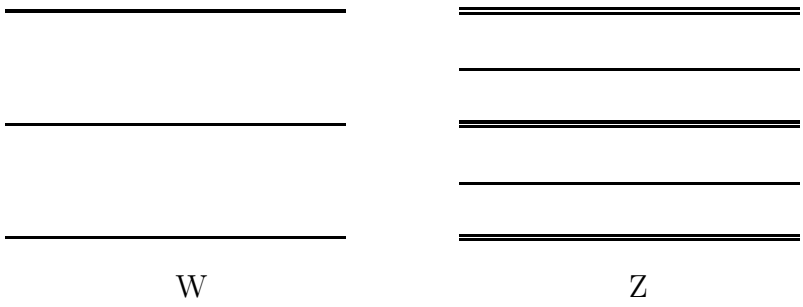

Figure 3: Schematic comparison of the $W^{\pm}$ and Z KK mass spectra showing that the $W^{\pm}$ KK states have masses almost identical to those of the degenerate pair of Z KK excitations.

Thus, determining the roots $x_1^W(\kappa)$ from the analysis discussed above, yields

$$x_1^Z(\kappa) = \frac{M_Z}{M_W} x_1^W(\kappa)\,, \tag{42}$$

with the ratio M_Z/M_W taken as exactly known. Note that we identify the lightest massive neutral KK state with the Z boson observed at LEP/SLC. In order to solve the Z_n eigenvalue equation (26), we input our chosen value of κ and our determined value of δ_L from which we can obtain δ_Y; λ remains an independent variable, but we pick its value in order to obtain the correct root x_1^Z above. Once this is accomplished, all of the electroweak parameters in the model (except κ) are completely determined, in particular, the Z_n KK tower masses and the wavefunction coefficients $a_{R,B}$ and $b_{L,R,B}$ of Eq. (19).

The masses of the Z_n KK tower states have an unusual behavior; there is a repeating pattern of a pair of almost degenerate states, followed by a single state, *e.g.*, the states Z_2 and Z_3 have a mass splitting of only 1%, Z_4 has no other nearby states, $Z_{5,6}$ are nearly degenerate, and so forth. In addition, the pair of states become more degenerate as the KK mode number increases. This KK mass spectrum is more easily understood by examining Figs. 2 and 3, where the W and Z KK spectra are displayed. Note that the W KK tower has a conventional mass spectrum, and each W KK mode coincides with the pair of degenerate Z KK states.

The couplings of the SM fermions to the massive Z_n KK tower states can be written in the suggestive form

$$\frac{g_{Z_n}}{c_w}(T_{3L}^f - s_n^2 Q^f)\,, \tag{43}$$

with $c_w = \cos\theta_w^{os}$ and $T_{3L}^f(Q^f)$ being the usual fermion third-component of weak isospin (electric charge). Matching with the form of the covariant derivative, the parameter s_n^2 is found to be given by

$$s_n^2 = \frac{-\lambda\chi_n^B(R)}{\chi_n^L(R) - \lambda\chi_n^B(R)}\,, \tag{44}$$

with $s_1^2 \equiv \sin^2\theta_{eff}$, *i.e.*, the value of the weak mixing angle obtained on the Z-pole. The values for s_n^2 vary significantly, even in sign, as the KK mode number varies. For example, for $\kappa = 3$, $s_2^2 = 0.743\,, s_3^2 = -0.109\,,$ and $s_4^2 = 0.218$. We note that for the KK levels which are non-degenerate, the value of s_n^2 is not too far from the on-shell value, $\sin^2\theta_w^{os} \simeq 0.22210$, as defined above. This can be understood as being due to the fact that the double states are mixtures of the γ and Z excitations, while the single states are almost pure Z excitations. Turning to g_{Z_n}, we know that in the SM $g_Z = g_W$, *i.e.*, $g_{Z_1} = g_{W_1}$ and it is traditional to define an effective ρ parameter [15]

$$\rho_{eff}^Z = \frac{g_{Z_1}^2}{g_{W_1}^2} = \frac{g_Z^2}{g_W^2}\,, \tag{45}$$

which can be directly calculated once the g_{Z_n} are known. Matching with the covariant derivative, we find that these couplings can be written as

$$\frac{g_{Z_n}^2}{c_w^2} = \Omega^2 g_{5L}^2 \frac{|\chi_n^L(R) - \lambda\chi_n^B(R)|^2}{N_{Z_n}}\,, \tag{46}$$

where Ω is determined numerically as discussed above. The normalization in the absence of brane kinetic terms is easily obtained,

$$N_{Z_n}^0 = 2\int_R^{R'} dz\,\frac{R}{z}\,\left\{|\chi_n^L(z)|^2 + |\chi_n^R(z)|^2 + |\chi_n^B(z)|^2\right\}\,, \tag{47}$$

with the factor of 2 being related to the interval of integration as described above. In order to determine N_{Z_n} in the more general case we must return to the two actions in Eqns. (3) and (4). To simplify the discussion, we first rescale each gauge field by its appropriate 5-d coupling, $A_i \to g_{5i}A_i$, and concentrate solely on the action integrands which we can combine and write symbolically as

$$-\frac{1}{4}F_L^2 - \frac{1}{4}F_R^2 - \frac{1}{4}F_B^2 - \frac{1}{4}F_C^2 - \frac{1}{4}(c_L F_L^2 + c_Y F_Y^2 + c_s F_C^2) r_c\delta(y)\,. \tag{48}$$

From this it is clear how to normalize fields [10] which are purely composed of A_L or A_C as in the case of the $W^\pm$ above. The difficulty with the remaining fields is that both the gauge fields and brane terms are a mixture of the two bulk fields as can be seen from the definition of Y in Eq. (16). Rewriting the Y fields in terms of A_R^3 and B, substituting the KK decomposition into the respective field strength tensors for the neutral fields, and neglecting the QCD terms, we see that symbolically

$$\begin{aligned}
&-\frac{1}{4}F_L^2 - \frac{1}{4}F_R^2 - \frac{1}{4}F_B^2 - \frac{1}{4}(c_L F_L^2 + c_Y F_Y^2) r_c \delta(y) \rightarrow \\
&|\chi_L|^2 + |\chi_R|^2 + |\chi_B|^2 + c_L r_c |\chi_L|^2 \delta(y) + c_Y r_c \left| \frac{g_{5R}\chi_B + g_{5B}\chi_R}{\sqrt{g_{5R}^2 + g_{5B}^2}} \right|^2 \delta(y) \qquad (49) \\
&= |\chi_L|^2 (1 + c_L r_c \delta(y)) + |\chi_R|^2 + |\chi_B|^2 + c_Y r_c \left| \frac{\kappa\chi_B + \lambda\chi_R}{\sqrt{\kappa^2 + \lambda^2}} \right|^2 \delta(y) \,.
\end{aligned}$$

Allowing for the extension of the integration range, this gives

$$\begin{aligned}
N_{Z_n} &= \int_R^{R'} dz \frac{R}{z} \left\{ |\chi_L^n(z)|^2 (2 + c_L r_c \delta(z-R)) + 2|\chi_R^n(z)|^2 + 2|\chi_B^n(z)|^2 \right. \\
&+ \left. c_Y r_c \frac{|\kappa\chi_B^n(z) + \lambda\chi_R^n(z)|^2}{\kappa^2 + \lambda^2} \delta(z-R) \right\} , \qquad (50)
\end{aligned}$$

which reduces to the result above when the c_i are neglected. Note that this expression also tells us how to normalize the photon field, which is a constant (*i.e.*, z-independent) with the substitutions $\chi_L^\gamma = \alpha_L \,, \chi_R^\gamma = \alpha_L/\kappa$, and $\chi_B^\gamma = \alpha_L/\lambda$. We will return to this point below. Given N_{Z_n}, the $g_{Z_n}^2$ are calculable and ρ_{eff}^Z can be directly determined; we find that in all cases $|\rho_{eff}^Z - 1| \lesssim 10^{-4}$. As in the case of the W KK tower, these couplings are observed to decrease rapidly as the KK mode number increases. For example, if $\kappa = 3$, the first KK excitation above the Z has a coupling strength which is only $\sim 11\%$ of the SM Z boson.

Returning to the case of the photon, we note from the form of the covariant derivative that it couples as

$$\begin{aligned}
&g_{5L} T_{3L}^f \chi_L^\gamma + g_{5R} T_{3R}^f \chi_R^\gamma + g_{5B} \frac{B-L}{2} \chi_B^\gamma \\
&= g_{5L} \alpha_L \left(T_{3L}^f + T_{3R}^f + \frac{B-L}{2} \right) \equiv g_{5L} \alpha_L Q^f \,, \qquad (51)
\end{aligned}$$

apart from a normalization factor which can be determined directly from N_{Z_n} above, giving

$$N_\gamma = 2\pi r_c \alpha_L^2 \left(\frac{\kappa^2 + \lambda^2 + \kappa^2\lambda^2}{\kappa^2\lambda^2} \right) \left\{ 1 + \frac{1}{\pi k r_c} \frac{\kappa^2\lambda^2\delta_L + (\kappa^2 + \lambda^2)\delta_Y}{\kappa^2 + \lambda^2 + \kappa^2\lambda^2} \right\} . \tag{52}$$

We thus obtain the α_L independent quantity

$$e^2 \equiv \frac{g_{5L}^2 \alpha_L^2}{N_\gamma} , \tag{53}$$

from which we can define the mixing angle

$$\sin^2\theta_{eg} \equiv \frac{e^2}{g_{W_1}^2} , \tag{54}$$

where $g_{W_1}^2$ has been previously defined.

Note that in the above discussion we have introduced three different definitions of the weak mixing angle: (i) the on-shell value $\sin^2\theta_w^{os}$, (ii) the effective value on the Z-pole, $\sin^2\theta_{eff}$, and (iii) $\sin^2\theta_{eg}$. In the SM, *at tree-level*, the values of these three definitions are, of course, equivalent. In the WHM, they need not be in general; however, if the model is to be consistent with experiment, it is clear that these three quantities must be reasonably close numerically. Fig. 4 shows these three definitions of $\sin^2\theta_w$ as functions of the parameter κ, where $\sin^2\theta_w^{os}$ is, of course, κ independent. From this figure, we see that as κ increases the three values of $\sin^2\theta_w$ merge together. This is due to the KK masses becoming heavier as well as the strengthening of the $SU(2)_R$ couplings associated with the custodial symmetry which forces the WHM to become more like the SM. Clearly, for values of $\kappa \simeq 3-4$, the three definitions of the weak mixing angle are quite close numerically. It is interesting to note that this model predicts $\sin^2\theta_{eff}$ to be somewhat smaller than the on-shell value, *e.g.*, for $\kappa = 3$, $\sin^2\theta_w^{os} - \sin^2\theta_{eff} \simeq 0.0006$. This slightly lower value of $\sin^2\theta_{eff}$ is suggestive of the low value obtained from LEP and SLD [2] from measurements of the leptonic couplings of the SM Z.

Before we further discuss the electroweak parameters in the next section, we will conclude this section by examining the KK tower associated with the gluon. In analogy to the case of the photon, the massless gluon zero-mode has a flat, z-independent wavefunction. This implies that the conventional strong coupling can be defined directly via the zero-mode

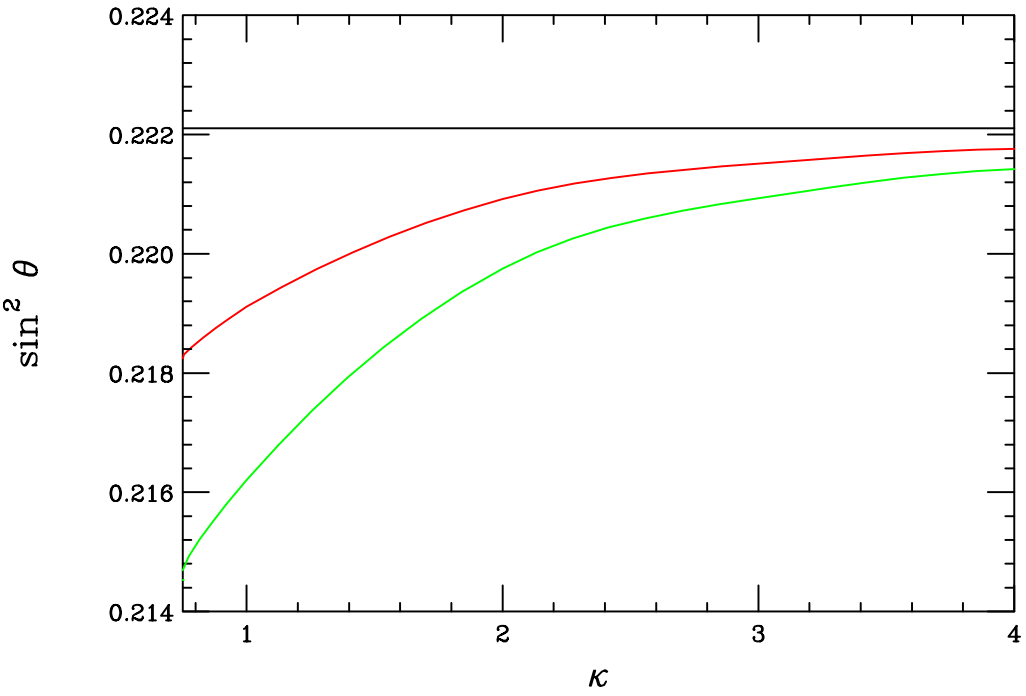

Figure 4: $\sin^2\theta$ in each of the three definitions as a function of κ. The black (upper), red (middle), and green (lower) curves correspond to the schemes $\sin^2\theta_w^{os}$, $\sin^2\theta_{eff}$, and $\sin^2\theta_{eg}$ defined in the text.

coupling to fermions following from the boundary conditions and the KK decomposition. We thus can write

$$g_s^2 = \frac{g_{5s}^2}{2\pi r_c Z_0}\,, \tag{55}$$

where

$$Z_0 = 1 + \frac{c_s}{2\pi} = 1 + \frac{\delta_s}{\pi k r_c}\,. \tag{56}$$

Note that to maintain $Z_0 > 0$, $\delta_s \geq -\pi k r_c$ is required. Solving for g_{5s}^2 we obtain

$$g_{5s}^2 = \frac{2\pi r_c g_s^2}{1 - g_s^2/\tilde{g}_s^2}\,, \tag{57}$$

so that

$$\delta_s = \pi k r_c \frac{g_s^2}{\tilde{g}_s^2 - g_s^2}\,. \tag{58}$$

Since $1/\tilde{g}_s^2 = 1/\tilde{g}_L^2 \cdot (\beta_s/\beta_L)$ is known, δ_s can be directly calculated. Taking $\alpha_s = 0.118$ we

obtain

$$\delta_s \simeq -29.14\,, \tag{59}$$

independent of κ.

Knowing the value of δ_s, we can now determine the gluon KK spectrum. Note that this value of δ_s is not far away from the critical region of $\delta = -\pi k r_c \simeq -35.4$ discussed above, where the KK spectrum and couplings become highly perturbed as shown in our earlier work [10]. In fact, for $\delta_s \leq -\pi k r_c$, the system becomes unphysical as ghost states appear. For the value of δ_s computed above, the first gluon KK excitation, g_1, is pushed upwards in mass by $\simeq 10\%$ in comparison to what would be naively expected for smaller values of the brane term, and hence m_{g_1} is roughly 200 GeV heavier than the first gauge KK excitation. The mass splitting for the higher gluon KK states are similar to those of the W KK tower.

The couplings of the gluon KK tower states can be directly calculated as in the W and Z cases above from the covariant derivative,

$$\frac{g_{s_n}^2}{g_s^2} = 2\pi r_c Z_0 \frac{|\chi_n^C(R)|^2}{N_{s_n}}\,, \tag{60}$$

where

$$N_{s_n} = \int_R^{R'} dz\, \frac{R}{z} |\chi_n^C(z)|^2 [2 + c_s r_c \delta(z-R)]\,. \tag{61}$$

Here, we note that $g_{s_0}^2 = g_s^2$, the usual QCD coupling. The coupling of the first gluon KK state is displayed as a function of the strong brane term in Fig. 5, where we see that the KK states of the gluon are more strongly coupled, scaled to the zero-mode coupling strength, as compared to the other KK towers. For the higher KK levels, the ratio $g_{s_n}^2/g_s^2$ does not decrease as quickly as in, *e.g.*, the case of the corresponding W boson KK tower couplings. For example, $g_{s_2}^2/g_s^2 \simeq 0.233$, while we previously found $g_{W_2}^2/g_W^2 \simeq 0.043$. This is due to the large magnitude of δ_s.

4 Electroweak Oblique Parameters

As discussed in the previous section, the WHM leads to a complete determination of the couplings of the $W\,, Z$ and gluon (as well as their KK towers) as a function of κ. We showed that the gauge boson zero-mode couplings to fermions are slightly different from their

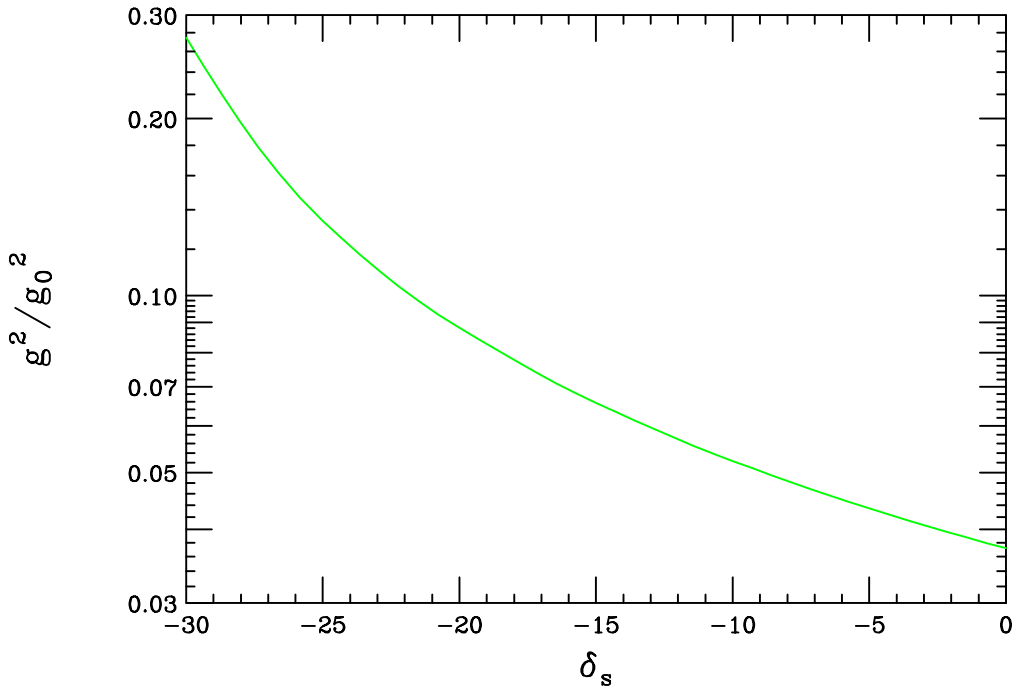

Figure 5: Behavior of the coupling of the SM quarks to the first gluon KK excitation as a function of the brane term δ_s, demonstrating the rapid growth in the coupling as $\delta_s \to -\pi k r_c$.

corresponding tree-level values in the SM, resulting in shifts from the SM expectations for the precision electroweak observables. These shifts can be approximately described through the oblique variables S, T, and U [16] even though the modifications do not arise from loop corrections. Shifts induced at tree-level occur for other new physics sources as well, and have been analyzed, *e.g.*, for the case of a simple Z' model [17].

We take α, M_Z, and G_F to be input parameters in performing our fit to the electroweak measurements, and hence a relevant set of observables to use in the fit is M_W, $\sin^2\theta_{eff}$, and Γ_ν, the width for $Z \to \nu\bar{\nu}$, which is essentially the invisible width of the Z. The explicit dependence of these observables on the oblique parameters is given by [16, 18]

$$\begin{aligned} \sin^2\theta_{eff} &= \sin^2\theta_0 + \frac{\alpha\Delta S}{4(c_w^2 - s_w^2)} - \frac{c_w^2 s_w^2 \alpha\Delta T}{c_w^2 - s_w^2}\,, \\ M_W^2 &= M_{W_{SM}}^2 \left[1 - \frac{\alpha\Delta S}{2(c_w^2 - s_w^2)} + \frac{c_w^2 \alpha\Delta T}{c_w^2 - s_w^2} + \frac{\alpha\Delta U}{4 s_w^2}\right]\,, \\ \Gamma_\nu &= \Gamma_{\nu_{SM}}(1 + \alpha\Delta T)\,, \end{aligned} \tag{62}$$

where α is the fine-structure constant. We write $\Delta S(T, U)$ as shifts in these parameters away

from their exact value at tree-level in the SM. Since we are comparing with the SM at tree-level we have $\sin^2\theta_0 = \sin^2\theta_w^{os}$. The ratio $\Gamma_\nu/\Gamma_{\nu_{SM}}$ is equal to ρ_{eff}^Z, using the notation of the previous section. Lastly, we have again imposed the requirement that M_W be in agreement with its SM value as defined by experiment, so that the oblique contribution in brackets on the right-hand side of the equation must vanish, thus forcing a relationship between the oblique parameters. Since for all values of κ, ρ_{eff}^Z is found to differ from unity only at the order of a few $\times 10^{-5}$, it is clear that ΔT is very small. The expression for M_W then yields

$$\Delta U \simeq \frac{2s_w^2}{c_w^2 - s_w^2}\,\Delta S\,. \tag{63}$$

Using the values of ρ_{eff}^Z computed above and $\sin^2\theta_{eff}$ from the previous section, we can determine all of the oblique parameters as a function of κ. This is displayed in Fig. 6. Here, we see that ΔT is very small as expected, ΔU tracks ΔS, and ΔS falls rapidly in magnitude as κ increases, as expected.

The most recent fit to the oblique parameters has been performed by Erler [19] using the data presented at the 2003 summer conferences [2]. The results for this fit are highly correlated; using $m_H = 117$ GeV, Erler obtains the 1σ constraints $S = -0.13 \pm 0.10$, $T = -0.17 \pm 0.12$ and $U = 0.22 \pm 0.13$. Slightly negative values of S, T are favored while the fit prefers slightly positive values of U. Comparing these results with the figure, we see that the WHM agrees well with the data for $\kappa \gtrsim 3$.

We recall that at loop level, S, T, and U are traditionally determined from the gauge boson self-energies [16]. Loop contributions are of order α, so they may also be important compared to the tree-level values discussed above. To leading order in $1/(\pi k r_c)$ the wavefunctions of the $W_1^\pm$ and Z_1 are flat in z, so we can calculate loop contributions in this approximation; the corrections will be of order $\alpha/(k\pi r_c) \simeq 2 \times 10^{-4}$, and can be safely ignored. For the photon, of course, the wavefunction is flat to all orders. The coupling of an approximately flat zero-mode to two excited modes is then given by, *e.g.*,

$$g_{5L}\Omega \int_R^{R'} dz\, \frac{R}{z}\, \frac{\chi_1^Z \chi_n^W \chi_m^W [2 + c_L r_c \delta(z-R)]}{(N_{Z_1} N_{W_n} N_{W_m})^{1/2}} = g_{5L}\delta_{nm} \tag{64}$$

by the orthonormality condition in Ref. [10]. This means that the couplings of the KK W modes (which participate in the loop of the γ/Z self-energy diagram) to the exterior Z or

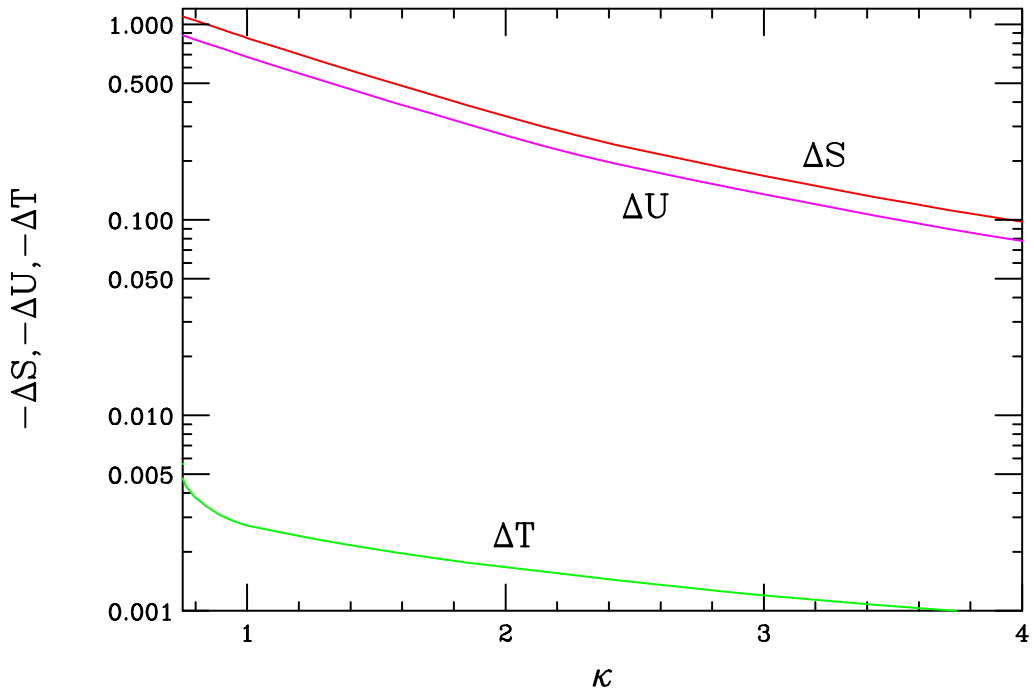

Figure 6: Shifts in the values of the oblique parameters S, T, and U as a function of κ from the tree-level analysis discussed in the text.

γ are exactly the same as the SM triple gauge couplings in this limit. In particular, the coupling of an excited W to the hypercharge boson is zero. We can write S as [20]

$$S = -16\pi \left. \frac{\partial \Pi_{ZY}(q^2)}{\partial q^2} \right|_{q^2=0}, \tag{65}$$

where $\Pi_{ZY}(q^2)$ is the self-energy mixing between the Z and the hypercharge boson (in this example) through W loops. So we conclude that, at order α, $\Delta S = 0$. We also expect the contribution to T to be small due to the presence of the custodial symmetry and because the mass splittings between the excited W and Z bosons are small. Hence the KK loop contributions to the oblique parameters can be safely ignored.

A more serious problem arises from the fact that the Higgs boson is no longer in the spectrum, and hence can not run in loops. To correctly estimate the one loop values of S, T, and U, one would need a procedure for systematically removing the effects of the Higgs loops from the precision electroweak observables. It is not clear how this can be accomplished easily, due to the non-gauge invariant nature of the relevant graphs.

It is also possible that there are higher dimension operators localized on the TeV

brane that violate S, since there is no symmetry to prevent them (T is protected by the custodial SU(2)). The size of these operators will naively be $M_Z^2/\Lambda_\pi^2 \approx 10^{-4}$, leading to contributions to S of order $\frac{1}{\alpha} M_Z^2/\Lambda_\pi^2 \approx 10^{-2}$.

In Ref. [21], the precision electroweak constraints on the WHM model, within a less general parameter space, were considered. Qualitatively, we agree with their conclusion that in the regime where many KK modes lie below the IR cutoff scale $\sim \Lambda_\pi$ of the warped space (corresponding to the regime of weakly interacting distinct states), the WHM is excluded by precision electroweak data. In our approach, a similar conflict arises between the electroweak data and unitarity, where the former requires the absolute scale of higher KK modes to lie above ~ 2 TeV, and the latter demands the opposite.

5 Unitarity in Gauge Boson Scattering

An important function of the Higgs boson in the SM is to insure the unitarity of the broken gauge theory. In this Higgsless model, we would like to test the claim in Ref. [5, 6] that the KK modes will be able to insure the unitarity in place of the Higgs.

The classic test of unitarity is the elastic scattering of two longitudinally polarized gauge bosons, $W_L W_L \to W_L W_L$ [22]. This amplitude receives tree-level contributions from the four W vertex, and from the three boson vertices through exchange of a single neutral gauge boson in the s- and t-channels, as shown in Fig. 7. The diagram involving the four boson vertex contains terms that grow like s^2, s and s^0, as well as innocuous terms involving powers of $1/s$. For the scattering to respect unitarity, the terms that grow with s must cancel against those arising from other graphs in the theory. Csaki *et al.* [5] have investigated the behavior of these terms at large s. Strictly speaking, the expansion they performed is only valid at energies 'above' all the KK masses. In practice, however, it is a good approximation to take values of $\sqrt{s}$ above a sufficiently large number of KK modes. In that region, it was shown in Ref. [5], that there are two necessary conditions for the terms which grow with energy in the 4-point contribution to be cancelled by those from the one-boson exchange

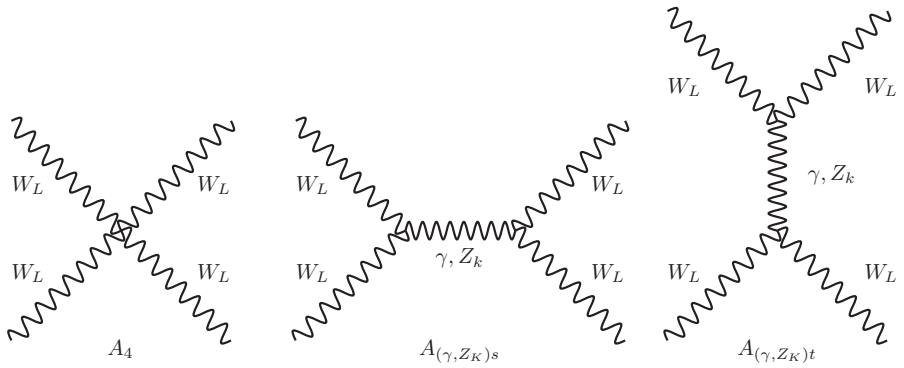

Figure 7: Feynman diagrams for the tree-level amplitudes contributing to $W_L W_L$ scattering.

graphs:

$$g^2_{nnnn} = \sum_k g^2_{nnk}\,,$$
$$4g^2_{nnnn}M_n^2 = 3\sum_k g^2_{nnk}M_k^2\,. \tag{66}$$

Here g^2_{nnnn} is the coupling of four gauge bosons with KK-number n, and g_{nnk} is the three boson coupling between two states with KK-number n and one with KK-number k. The first of these conditions insures the cancelling of terms in the amplitude that grow like s^2, and is guaranteed by the original gauge invariance. The second condition is required for the cancellation of the terms that grow like s, and it is not trivial that it will be satisfied in the present model. For the case of ordinary W scattering, $n = 1$.

To test these conditions we have examined numerically the case of $W_L^+ W_L^-$ scattering, since this is an important process, and will be measured at future colliders. The relevant couplings are given by

$$g^2_{1111} = g^2_{5L}\Omega^2 \int_R^{R'} dz\, \frac{R}{z}\, \frac{1}{N^2_{W_1}} \left(|\chi_1^{L^\pm}|^4 [2 + c_L r_c \delta(z-R)] + 2\kappa^2 |\chi_1^{R^\pm}|^4 \right)\,, \tag{67}$$
$$g_{11k} = g_{5L}\Omega \int_R^{R'} dz\, \frac{R}{z}\, \frac{1}{N_{W_1}\sqrt{N_{Z_k}}} \left(|\chi_1^{L^\pm}|^2 \chi_k^{L^0} [2 + c_L r_c \delta(z-R)] + 2\kappa |\chi_1^{R^\pm}|^2 \chi_k^{R^0} \right)\,,$$

where N_{W_1} and N_{Z_k} are the normalization factors given above. For the first sum rule we also need the coupling of two $W_1^\pm$ bosons to the photon, which is just e by gauge invariance.

We have numerically evaluated g^2_{1111} and g_{11k} for k ranging over the photon, the Z_1, and the first 9 higher excited states. The agreement with the sum rules is quite good, and

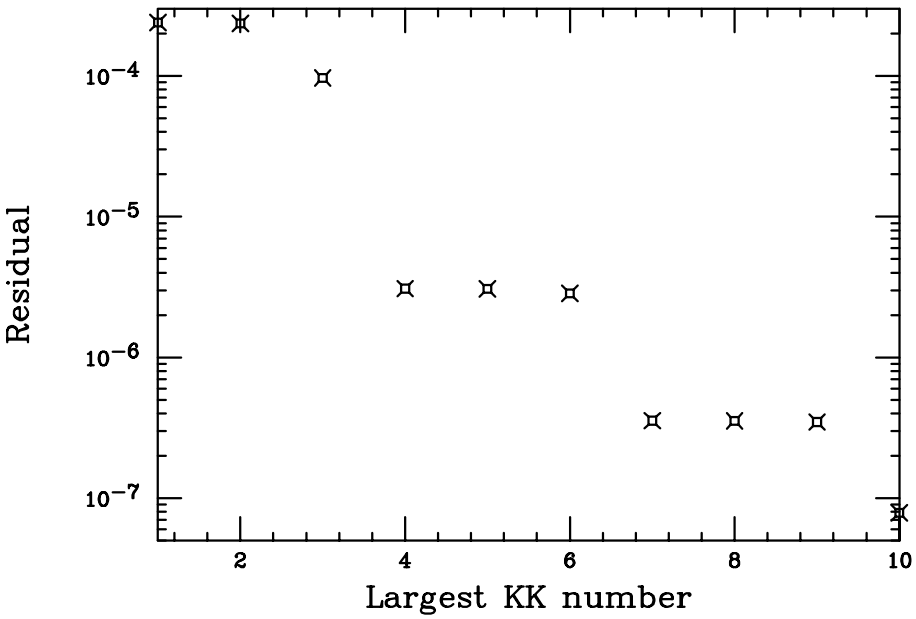

Figure 8: The residual of the sum rule $1 = \sum_k g_{11k}^2/g_{1111}^2$ as a function of the highest KK state included in the sum. This shows that the sum rule is converging, and hence the cross section will behave like $1/s$ at asymptotically large $\sqrt{s}$.

was observed to rapidly improve as more states were added. The residuals of these sum rules after including the first 9 excited states are

$$1 - \sum_{k=\gamma,1}^{10} \frac{g_{11k}^2}{g_{1111}^2} = 7.85 \times 10^{-8}\,,$$

$$1 - \frac{3}{4}\sum_{k=1}^{10} \frac{g_{11k}^2}{g_{1111}^2}\frac{M_{Z_k}^2}{M_{W_1}^2} = 1.96 \times 10^{-3}. \tag{68}$$

This shows that the sum rules are being satisfied, and so in the asymptotic region the cross section will indeed fall like $1/s$. The convergence of these sums as more KK states are added can be seen in Fig. 8.

The sum rules, however, are necessary, but not sufficient conditions for unitarity. In particular, the amplitude for $W_L^+W_L^-$ scattering, which grows like s^2 near a few times M_W^2, could grow too large before sufficiently many KK modes are passed. There is also a term formally independent of s, the coefficient of which could grow as more and more KK modes are included. It is possible that this term will also contribute to unitarity violations. To investigate this issue we examine the full amplitude for $W_L^+W_L^-$ scattering.

The amplitudes due to photon and Z exchange have been previously computed. Simple modifications of the formulae in Ref. [23] gives

$$\begin{aligned}
A_{s\gamma} &= -\frac{1}{16} i e^2 s^2 \beta^2 (3-\beta^2)^2 \cos\theta \,, \\
A_{sZ_k} &= -\frac{1}{16} i g_{11k}^2 \frac{s^3}{s-\xi_{Z_k}} \beta^2 (3-\beta^2)^2 \cos\theta \,, \\
A_{t\gamma} &= -\frac{ie^2 s^3}{32t} \left[\beta^2(4-2\beta^2+\beta^4) + \beta^2(4-10\beta^2+\beta^4)\cos\theta \right. \\
&\quad \left. + (2-11\beta^2+10\beta^4)\cos^2\theta + \beta^2\cos^3\theta \right] \,, \\
A_{tZ_k} &= -\frac{i g_{11k}^2 s^3}{32(t-\xi_{Z_k})} \left[\beta^2(4-2\beta^2+\beta^4) + \beta^2(4-10\beta^2+\beta^4)\cos\theta \right. \\
&\quad \left. + (2-11\beta^2+10\beta^4)\cos^2\theta + \beta^2\cos^3\theta \right] \,, \\
A_4 &= -\frac{1}{16} i g_{1111}^2 s^2 (1+2\beta^2-6\beta^2\cos\theta-\cos^2\theta) \,,
\end{aligned} \tag{69}$$

where $\xi_{Z_k} = M_k^2/M_W^2$, $t = -\frac{1}{2}s\beta^2(1-\cos\theta)$, and $\beta = \sqrt{1-4/s}$, and the labels refer to s and t-channel exchanges. Here s and t have been scaled to M_W^2. As is well known, in the SM the sum of these amplitudes grows like s. This growth is cancelled by the Higgs contributions

$$\begin{aligned}
A_{sH} &= -\frac{1}{16} i g^2 s^2 (1+\beta^2)^2 \frac{1}{s-\xi_H} \,, \\
A_{tH} &= -\frac{1}{16} i g^2 s^2 (\beta^2-\cos\theta)^2 \frac{1}{t-\xi_H} \,,
\end{aligned} \tag{70}$$

with $\xi_H = m_H^2/m_W^2$.

As we have seen, in the present model, the terms growing with s are cancelled at large s by the sum over the KK modes. For intermediate regions of s we investigate the full amplitude

$$A = A_4 + A_{s\gamma} + A_{t\gamma} + \sum_{k=1}^{\infty} \left(A_{sZ_k} + A_{tZ_k} \right) \,. \tag{71}$$

For reference, the cross section, with a cut on the scattering angle $|\cos\theta| \le z_0$, is

$$\sigma = \frac{1}{16\pi s^2 \beta^2} \int_{t_-}^{t_+} dt \, |A|^2 \,, \tag{72}$$

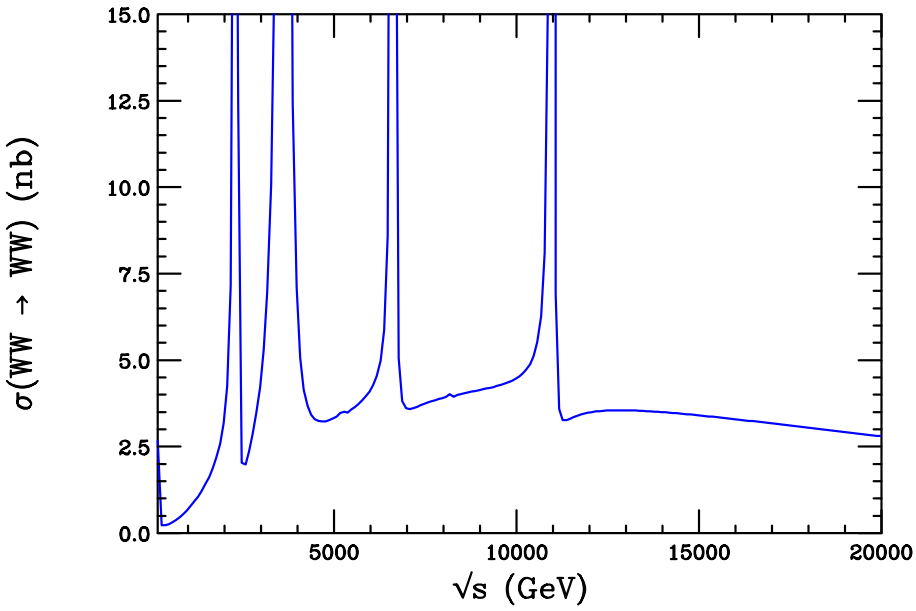

Figure 9: The cross section for $W_LW_L \to W_LW_L$ scattering with the first 10 KK states included. A heavy fake state has also been included with a mass of 14.7 TeV and coupling $g = 2.8 \times 10^{-4} g_{1111}$ to complete the sum rules and show that the cross section falls like $1/s$ asymptotically. No attempt has been made to smooth the poles at the KK resonances.

with $t_\pm = (2 - \frac{1}{2}s)(1 \mp z_0)$. This cross section, summed over the first 10 KK modes, is shown in Fig. 9, taking $z_0 = 0.98$. To demonstrate the asymptotic behavior, we have inserted a heavy fake state with mass and coupling chosen ($m_{heavy} = 14.7$ TeV and coupling $g = 2.8 \times 10^{-4} g_{111}$) to cancel the residuals in Eq. (68). This heavy fake state is intended to numerically compensate for extending the KK sum out to infinity. When this state is included, the cross section is seen to fall like as expected. However, it is clear that while including 10 KK states is enough to flatten the cross section, as seen in the region below the fake state, it is not enough to make it fall with s.

A good test of the unitarity of this scattering process is that the first partial wave amplitude should be bounded for all s [22]

$$|\mathcal{R}e\,(a_0)| = \left|\mathcal{R}e\left(\frac{1}{32\pi}\int_{-1}^{1} d\cos\theta(-iA)\right)\right| \leq \frac{1}{2}. \tag{73}$$

We have calculated this quantity for the amplitude in Eq. (71), again summing over the first 10 KK modes. Our result is shown in Fig 10. Unitarity is clearly violated at a center of mass energy of $\sqrt{s} \approx 2.0$ TeV, below the mass of the first KK mode. Note that this is only slightly better than the value obtained for the 4-d Standard Model without a Higgs, where

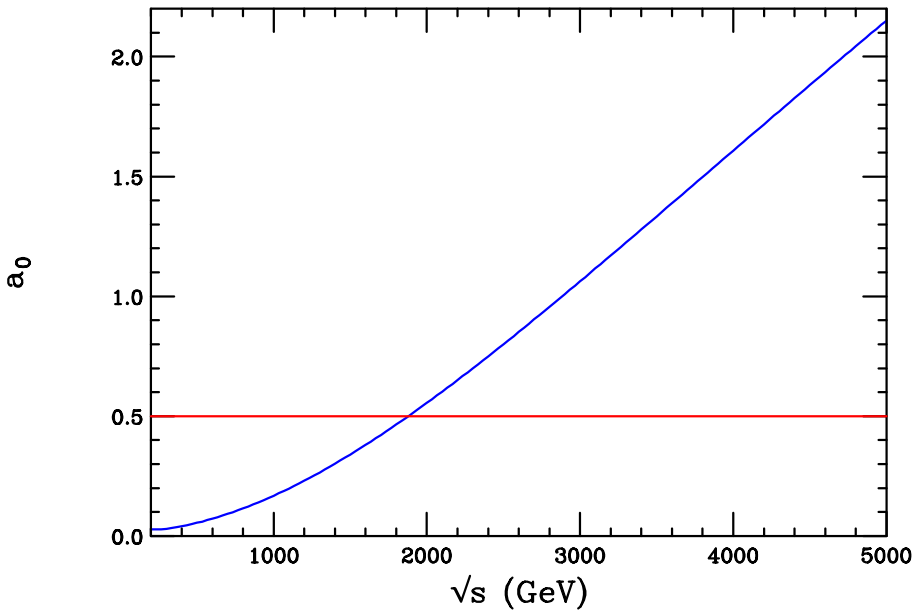

Figure 10: The real part of the zeroth partial wave amplitude for $W_L W_L \to W_L W_L$ scattering as a function of $\sqrt{s}$. The first 10 KK states have been included. Unitarity is violated if this amplitude exceeds $1/2$, which is seen to occur at $\sqrt{s} \approx 2$ TeV.

unitarity breaks down at $\sqrt{s} \approx 1.7$ TeV. The problem can be traced to the fact that the first higher excited modes are too heavy to have much influence before unitarity is violated. So, while the cross section will behave like $1/s$ at *asymptotically* high energies, unitarity is violated before that regime sets in.

For comparison we have performed the same calculation for the equivalent theory in flat space (with $\kappa = 1$), as presented in Section 6 of Ref. [5]. Our results are shown in Fig. 11. In that case, the first excited mode sits at 240 GeV, and the spacing between successive modes is 160 GeV. When $\sqrt{s}$ has reached a few TeV many KK modes have been passed and both sum rules are nearly saturated, so the terms growing with s are nearly cancelled. We thus see that the flat space equivalent theory is well-behaved.

It is possible that the WHM could be unitary if the masses of the higher excited modes were reduced. However, we have already seen that in this case the model is strongly excluded by precision electroweak data. We also note that the $W_L W_L$ scattering process can proceed by KK graviton exchange, and that this contribution has the opposite sign in the amplitude, so one might hope that unitarity could be restored by destructive interference between the gauge and gravity sectors. However, the ratio of the KK graviton to gauge exchange amplitudes is

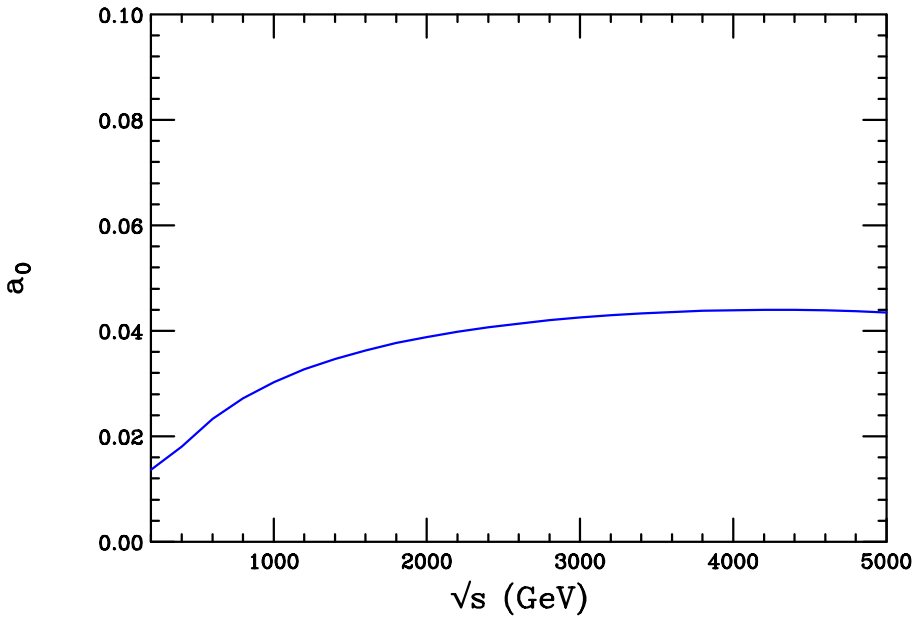

Figure 11: The real part of the zeroth partial wave amplitude for $W_L W_L \to W_L W_L$ scattering in the flat space equivalent of the WHM. The first 10 KK states have been included. Unitarity is violated if this amplitude exceeds $1/2$, which is seen to never occur. In this case the sum rules are almost saturated well before $\sqrt{s} = 1.7$ TeV, where the SM without a Higgs violates unitarity.

roughly $M_W^2/(g^2\Lambda_\pi^2) \approx 10^{-4}$, leading to a strong suppression. Numerically we find this effect to be insignificant. A similar situation holds for the contribution of the radion scalar, which is also present in the model. We thus conclude that this model is excluded in its present form.

6 Collider Signals

Thus far, we have seen that consistency with precision electroweak data demands that the ratio $\kappa = g_{5R}/g_{5L}$ take on larger values, such as $\kappa \sim 3$, which strongly enforces the custodial symmetry. We have also seen that unitarity in gauge boson scattering is problematic in the WHM model for such values of κ. Although the sum rules in Ref. [5], which are derived from the amplitude for longitudinal W scattering, are satisfied once enough gauge KK states are included, we demonstrated that the unitarity condition for the zeroth partial wave amplitude is violated for larger values of κ. Hence the WHM model is excluded in its present form. In this section, however, we will take the view that the model may be extended or modified,

	m_{Z_n} (TeV)	g_{Z_n}/g_{SM}	s_n^2
Z_2	2.30	0.106	0.743
Z_3	2.31	0.163	-0.109
Z_4	3.62	0.065	0.218
Z_5	5.24	0.072	0.748
Z_6	5.26	0.113	-0.104

Table 1: Mass spectrum and fermionic couplings for the first five excited neutral gauge KK states above the Z, taking $\kappa = 3$. The KK coupling strength is scaled to the SM weak coupling.

e.g., with the inclusion of additional non-Higgs states, in such a way as to restore unitarity. We thus examine the general collider signatures of the gauge and graviton KK states, as these are most likely a generic feature in any extended Higgsless model based on a warped geometry.

We first examine the signatures of the neutral gauge KK states, recalling that the mass spectrum of these states and their couplings to the SM fields are derived in Section 3. We will take $\kappa = 3$ throughout this section, in accordance with the constraints from precision electroweak measurements. The resulting spectrum and fermionic couplings for the first few excited neutral gauge KK states above the Z are displayed in Table 1, where the couplings are written in the form

$$\frac{g_{Z_n}}{c_w}(T_{3L}^f - s_n^2 Q^f)\,. \tag{74}$$

We see a general trend of decreasing coupling strength, g_{Z_n}, with increasing KK mode. These couplings are roughly $7-16\%$ (with the exact value depending on the mode number) of the SM weak coupling strength, and hence we can expect smaller production rates for these states. In addition, we note that the pair of nearly degenerate states have different fermionic interactions due to the parameter s_n^2. Measuring these couplings would separate the two degenerate states and uniquely identify this model.

The classic mechanism for producing heavy neutral gauge bosons in hadronic collisions is Drell-Yan production, $pp \to Z_n \to \ell^+\ell^-$, where the Z_n appears as a resonance. The Drell-Yan lineshape is clearly dependent on the total width of the Z_n, which varies in the WHM depending on the placement of the fermions. We have thus allowed for the total width of

the nth gauge KK state to float,

$$\Gamma_n = c\,\Gamma_n^0\,, \tag{75}$$

where Γ_n^0 corresponds to the case where all the SM fermions reside on the Planck brane. We have taken the range $1 \leq c \leq 100$, which accomodates for the possibility, *e.g.*, that the third generation fermions are in the bulk and are localized far from the Planck brane. The resulting event rate, in the electron channel only, for the nearly degenerate states $Z_{2,3}$ is displayed in Fig. 12 for the LHC with an integrated luminosity of 3 ab^{-1}. This high value of integrated luminosity corresponds to that proposed for the LHC upgrades [24]. The apparently isolated single resonance is, of course, a superposition of the Z_2 and Z_3 KK states. The effect of increasing the Z_n width is readily visible; the resonance peak becomes flattened if the total width is too large. However, it is clear that Drell-Yan production provides a clean discovery channel for the first two excited states in the case $\Gamma_n \lesssim 25\Gamma_n^0$. For present design luminosities, ~ 100 fb^{-1}, the event rate is simply scaled by a factor of 30 and the signal remains strong. The next excitation, Z_4, is very weakly coupled, and we have found that the corresponding peak is too small to be observed above the Drell-Yan SM continuum. The corresponding event rate for the higher mass KK states, $Z_{5,6}$, is also shown in Fig. 12, again assuming 3 ab^{-1} of integrated luminosity. Here, we see that the number of events is small, and even when the μ channel is also included these resonances are unlikely to be observed. Hence the LHC is likely to only observe a single resonance peak, corresponding to the superposition of the first two Z excitations. We also expect that only the first W excitation will be observable at the LHC. We note that the visible spectrum of the weak gauge KK states in the WHM at the LHC will appear similar to that from a flat extra dimension with brane terms. The KK states arising from flat space in the absence of brane terms will have a larger production rate [25], due to the larger couplings, and will be differentiable from the WHM.

In principle, neutral gauge KK production may be distinguished from that of more conventional extra gauge bosons arising in, *e.g.*, a GUT model [26]. The presence of the two nearly degenerate KK states (whether they be the $Z_{2,3}$ in the WHM, or the photon and Z KK excitations in flat space) results in a unique resonance shape, which is different from the case of a single new gauge state. In the present case, the Z_2 and Z_3 resonances destructively interfere with the SM background, yielding the dip in the line-shape in the invariant mass bins just below the heavy resonances. This effect is in principle measurable at the LHC [27], given enough statistics, and is a means for identifying the production of gauge KK states. In addition, the indirect exchange of the Z_n (for $\sqrt{s} < m_{Z_n}$) in fermion pair production in

e^+e^- annihilation results in a pattern of deviations in the cross sections and corresponding asymmetries which allows for the determination of the fermionic couplings of additional Z bosons [28]. In principle, a TeV class Linear Collider (LC) could thus be able to resolve the Z_2 from the Z_3 and separately measure their couplings. This claim should be verified by an independent study. A multi-TeV LC, such as CLIC, would be able to run on the resonance peaks, measure the individual line-shapes, and perform detailed studies of the couplings for each state.

The KK excitations of the gluon may be produced as resonances in dijet distributions at the LHC. The $2 \to 2$ parton-level subprocesses which contribute to dijet production are $q\bar{q} \to q\bar{q}\,, q\bar{q} \to gg\,, qg \to qg\,, gg \to gg\,,$ and $qq \to qq$. In principle, the gluon KK states can contribute via s-channel exchange in the $q\bar{q}$ and gg initiated processes, and via t- and u-channel exchange in $qg \to qg$ and $gg \to gg$. Here, we are only concerned with the search for peaks in the dijet invariant mass distribution, and hence neglect the possible gluon KK t- and u-channel contributions. Such contributions would, however, be revealed in dijet angular distributions. We are then left with computing the KK s-channel exchange diagrams, for which we need to first examine the gluon KK couplings to the SM fields. The expression for the $q\bar{q}g_n$ coupling is given in Eq. (60) and its strength is shown in Fig. 5 for the first excitation as the brane kinetic term is allowed to vary. For the value of the brane terms present in the WHM, the strength of the square of this coupling is $0.234\,(g_s^{SM})^2$ for the first gluon excitation and $0.143\,(g_s^{SM})^2$ for the second KK mode. These coupling strengths are a larger fraction of the usual SM value as compared to the corresponding couplings of the weak boson KK states due to the large negative value of δ_s. Recalling that the zero-mode gluon wavefunctions are flat in z, it is easy to see that the $g_0 g_0 g_1$ coupling is forbidden by orthonormality. Hence the gg initiated process does not contribute to the resonant production of the KK modes and the $q\bar{q} \to q\bar{q}$ subprocess is the only process we need to consider here. We also recall that the gluon KK mass spectrum tracks that of the W boson KK states with $m_{g_1} = 2.53$ TeV and $m_{g_2} = 5.51$ TeV.

The resulting event rate for the dijet invariant mass distribution is displayed in Fig. 13 for the first and second KK excitations, taking 100 fb^{-1} and 3 ab^{-1} of integrated luminosity, respectively. Here, we have employed the cuts $|\eta| < 1$ and $|p_T^{jet_1}| > 800(1500)$ GeV for the first (second) excitation. We see that the event rates are enormous and that both excitations will be observable at the LHC. Varying the width, as done above in the case of Drell-Yan production, will flatten the peak, but should not affect the visibility of the signal unless the

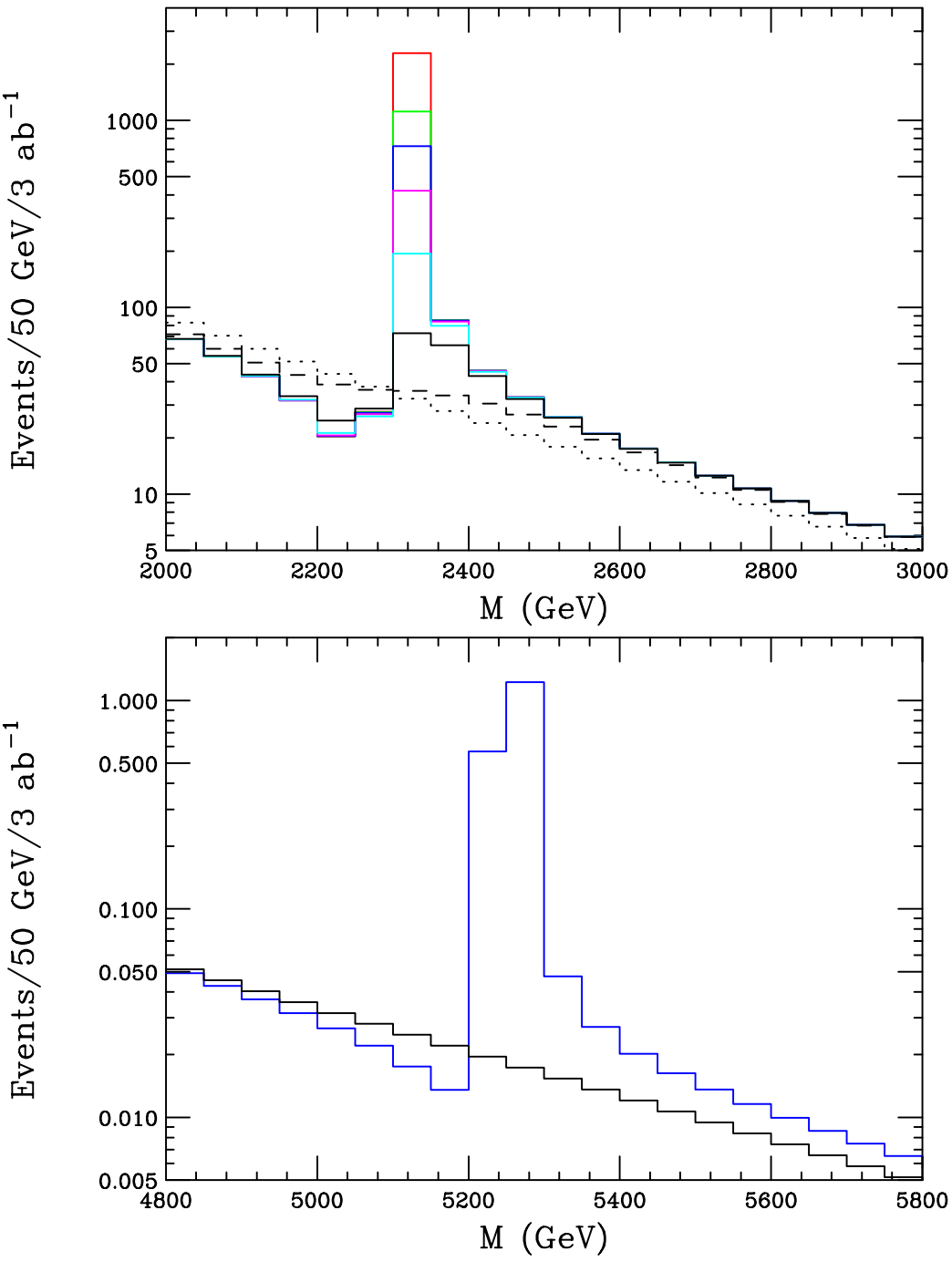

Figure 12: Top panel: Event rate for Drell-Yan production of the $Z_{2,3}$ gauge KK states, in the electron channel, as a function of the invariant mass of the lepton pair at the LHC with 3 ab^{-1} of integrated luminosity. The dotted histogram corresponds to the SM background, while the histograms from the top down (represented by red, green, blue, magenta, cyan, solid, and dashed) correspond to letting the width float with a value of $c = 1\,, 2\,, 3\,, 5\,, 10\,, 25\,, 100$. Bottom Panel: Event rate for Drell-Yan production of the $Z_{5,6}$ gauge KK states as a function of the invariant mass of the lepton pair at the LHC with 3 ab^{-1} of integrated luminosity (blue histogram). The bottom solid histogram corresponds to the SM background.

width grows very large. Observation of the first dijet resonance, in addition to the peak present in the Drell-Yan distribution, will signal that the full SM gauge sector resides in the bulk. The slightly different value of the mass for g_1, as compared to that for $Z_{2,3}$, with the g_1 being roughly 200 GeV heavier than the Z KK states, will signal that brane kinetic terms are present in the model. Given the large event rate for the production of these KK states, this mass difference should be measurable. Observation of the second gluon KK dijet peak will reveal the mass gap between the states in the KK tower, and will signal the presence of a warped, rather than flat, geometry. Hence, observation of the KK dijet resonances is critical to the identification of this model.

We now turn to the production of the graviton KK states and first consider the case of resonant graviton production. This is well-known to be the main signature of the original RS model [9]. In principle, resonant graviton production can proceed via $q\bar{q}$ and gg initiated subprocesses. However, in the WHM scenario where the fermions are localized on the Planck brane, the graviton KK tower couples to fermions with $\overline{M}_{Pl}^{-1}$ strength or smaller since no warp factor is generated in the coupling. Hence the graviton KK tower decouples from the fermion sector. Examining the couplings of the graviton excitations to the zero-mode vector bosons, we see that in the absence of brane terms these are given simply by [13]

$$g^0_{V_0V_0G_n} = \frac{2}{\Lambda_\pi \pi k r_c}\left(\frac{1-J_0(x_n^G)}{(x_n^G)^2|J_2(x_n^G)|}\right) , \tag{76}$$

where x_n^G denotes the roots which determine the graviton KK mass spectrum and, for example, $V_0 = g$. In the presence of brane kinetic terms, both the V_0 wavefunction and the $V_0V_0G_n$ interaction are modified; in the case $V_0 = g$,

$$g_{V_0V_0G_n} = \frac{N_{V_0}(\delta_i = 0)}{N_{V_0}}\left\{g^0_{V_0V_0G_n} + \cdots\right\} , \tag{77}$$

where δ_i denotes the appropriate brane term. The omitted terms in the bracket are proportional to $(x_n^G)^2 e^{-2\pi k r_c}$ for $n > 0$ and thus are negligible. Note that these terms are essential, however, to retain the $\overline{M}_{Pl}^{-1}$ behavior of the zero-mode graviton coupling. For the case of the graviton KK tower, the only influence of the brane terms on the $V_0V_0G_n$ coupling arises from modifications of the vector boson wavefunction.

Resonant graviton KK production thus proceeds through $gg \to G_n \to \gamma\gamma\,, gg\,, ZZ\,, WW$. Since the G_n coupling is significantly weaker than that for the gluon excitations, we expect

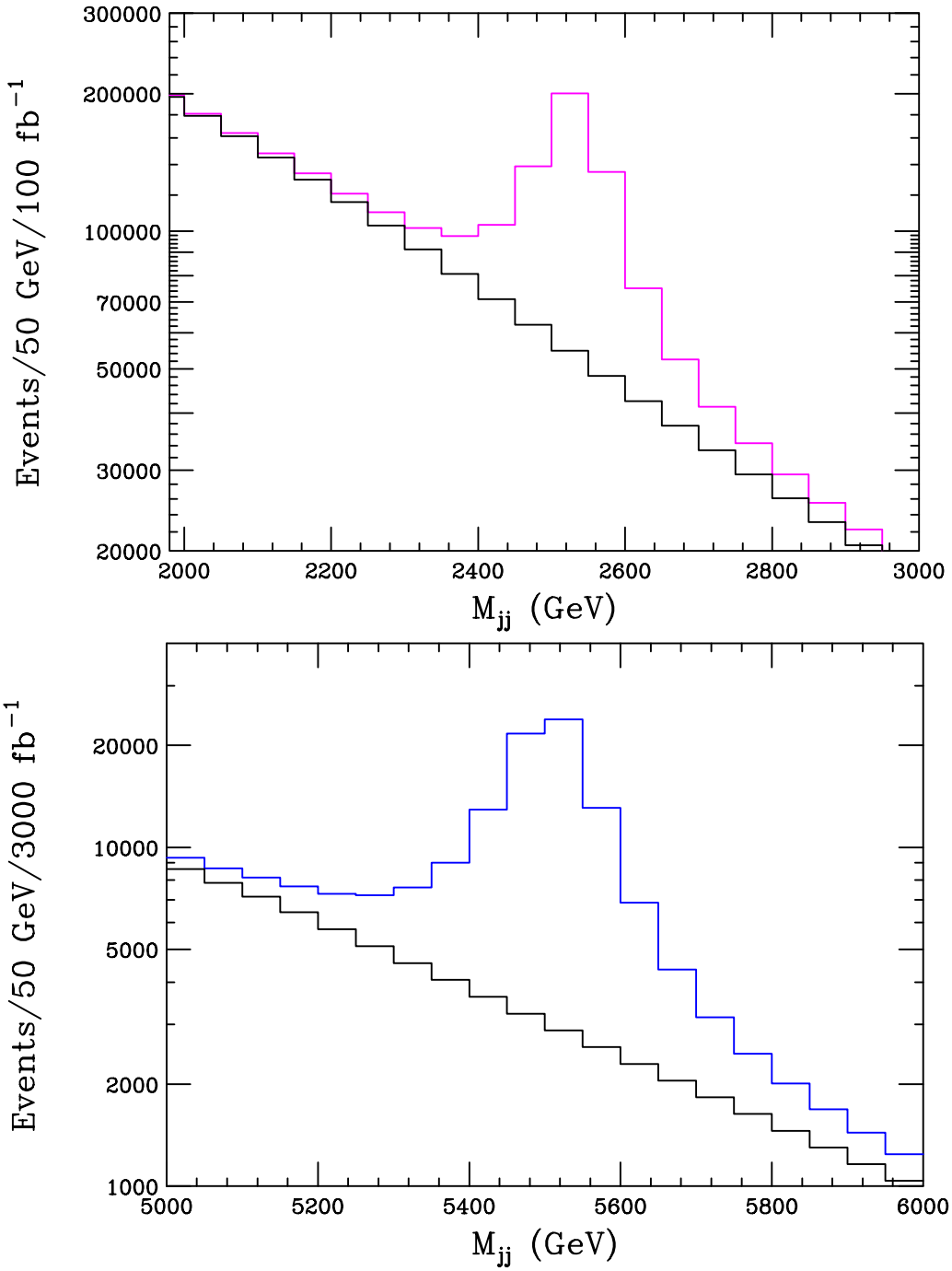

Figure 13: Production of the first (top panel) and second (bottom panel) gluon KK excitation in the dijet channel as a function of the dijet invariant mass. The SM background is given by the black histogram.

that the gg channel and ZZ, WW decay to hadronic final states will be overwhelmed by the SM background. Likewise, we expect the rate for the leptonic final states to be small due to the low ZZ, WW leptonic branching fractions. Thus, we only consider the $\gamma\gamma$ final state. The SM diphoton background arises from $q\bar{q} \to \gamma\gamma$ and $gg \to \gamma\gamma$, where the latter process proceeds through a box diagram. We include both of these SM processes in our background calculation. The event rate at the LHC, with 3 ab^{-1} of integrated luminosity, is displayed in Fig. 14 for the first graviton excitation and the SM background as a function of the diphoton invariant mass. In our numerical calculations, we assume $k/\overline{M}_{Pl} = 0.1$. We see that the G_1 production has a very small event rate and is indistinguishable from the background. Hence, the WHM differs from the usual RS scenario in that graviton resonances will not be observed.

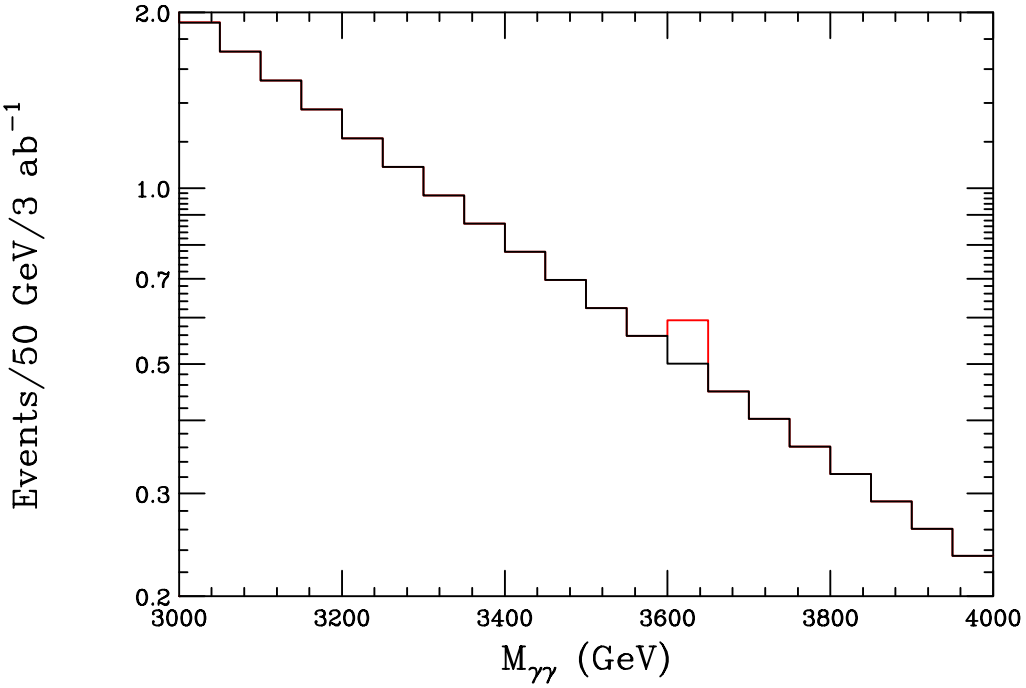

Figure 14: Production rate for the first graviton excitation at the LHC via the process $gg \to G_1 \to \gamma\gamma$ as a function of the diphoton invariant mass. The SM diphoton background is also shown. The two histograms are indistinguishable except for the small blip at $M_{\gamma\gamma} = m_{G_1}$

For completeness, we also considered the associated production of KK gravitons via $gg \to G_n + g$. Appropriately modifying the expressions in Ref. [29] for the WHM we computed the event rate at the LHC for G_1 production as a function of jet energy using an integrated luminosity of 3 ab^{-1}. We found that for typical jet energies of $E_j = 200$ GeV the cross section was of order 0.016 ab, and hence is also too small to be observed, even with

the proposed LHC luminosity upgrades. We thus conclude that in this model, the graviton KK tower can not be observed at high energy colliders.

Lastly, we note that there exists a radion scalar in this model and that it may have distinctive collider signatures.

7 Conclusions

Various phenomenological aspects of a Higgsless 5-d model [6], based on the RS hierarchy proposal [3], were studied in this paper. We considered independent left and right bulk gauge couplings and included the effects of brane localized kinetic terms for the gauge fields [7]. These terms were assumed to be radiatively generated, which is a generic expectation in orbifold models [12]. Our analysis was not limited to leading order bulk-curvature effects unlike in Refs. [6, 7], and also allowed for a more general set of parameters than that discussed in Ref. [21].

We computed the mass spectrum and the relevant couplings of the $W^{\pm}$ and γ/Z KK towers, and studied experimental constraints on the model parameters. Our main conclusion is that in the region of parameter space allowed by precision EW data, this model is not unitary at tree level above $\sqrt{s} \approx 2$ TeV, which is below the scale of the new KK states. Thus, to make reliable calculations based on the WHM, one must extend this model in order to unitarize the amplitudes. Setting the issue of unitarity aside, it was also observed that quantum contributions to the S, T, U oblique parameters [16, 18] are expected to be small. However, in the absence of the Higgs, regularization of the relevant loop diagrams may require non-renormalizable TeV brane counter terms whose coefficients are unknown. This imposes a degree of uncertainty on loop corrections. Further work regarding loop corrections is needed before more precise statements could be made in this regard.

Finally, we considered the collider signatures of the model, assuming that unitarity could somehow be restored without significantly modifying our numerical results. These signatures depend on the 5-d configuration of bulk fermions. We assumed a simple setup, where all fermions, except perhaps for the third generation, are localized near the Planck brane. The effect of different localizations of quarks was then taken into account by varying the widths of the KK resonances. Generically, we found that the low-lying gauge boson KK modes, including the gluons, would be observable, whereas the most distinct RS signature,

the spin-2 graviton KK resonances, would most likely evade detection at the LHC.

The AdS/CFT correspondence [4] provides a 4-d interpretation of this model in terms of strong dynamics. Thus, the tools and insights of both five and four dimensional model building can be employed in making this scenario more realistic such that it agrees with the SM at low energies. This setup provides an entirely higher dimensional explanation of the observed weak interaction mass scales, directly linking them to the IR scale in the RS model. Thus, it is worth the effort to find solutions for the problems that plague the present form of the WHM.

Acknowledgements We would like to thank Nima Arkani-Hamed, Tim Barklow, Graham Kribs, Hitoshi Murayama, and Michael Peskin for discussions related to this work.

References

[1] For a review of Higgs boson searches, see, M. Schmitt, talk given at the XXI International Symposium on Lepton and Photon Interactions at High Energies, Batavia, IL, August 2003.

[2] The LEP and SLD Electroweak and Heavy Flavor Working Groups, arXiv:hep-ex/0312023.

[3] L. Randall and R. Sundrum, Phys. Rev. Lett. **83**, 3370 (1999) [arXiv:hep-ph/9905221].

[4] J. M. Maldacena, Adv. Theor. Math. Phys. **2**, 231 (1998) [Int. J. Theor. Phys. **38**, 1113 (1999)] [arXiv:hep-th/9711200].

[5] C. Csaki, C. Grojean, H. Murayama, L. Pilo and J. Terning, "Gauge theories on an interval: Unitarity without a Higgs," arXiv:hep-ph/0305237.

[6] C. Csaki, C. Grojean, L. Pilo and J. Terning, "Towards a realistic model of Higgsless electroweak symmetry breaking," arXiv:hep-ph/0308038.

[7] Y. Nomura, "Higgsless theory of electroweak symmetry breaking from warped space," arXiv:hep-ph/0309189.

[8] C. Csaki, C. Grojean, J. Hubisz, Y. Shirman and J. Terning, "Fermions on an interval: Quark and lepton masses without a Higgs," arXiv:hep-ph/0310355.

[9] H. Davoudiasl, J. L. Hewett and T. G. Rizzo, Phys. Rev. Lett. **84**, 2080 (2000) [arXiv:hep-ph/9909255], Phys. Lett. B **473**, 43 (2000) [arXiv:hep-ph/9911262]. See also, A. Pomarol, Phys. Lett. B **486**, 153 (2000) [arXiv:hep-ph/9911294].

[10] H. Davoudiasl, J. L. Hewett and T. G. Rizzo, Phys. Rev. D **68**, 045002 (2003) [arXiv:hep-ph/0212279]. See also, M. Carena, E. Ponton, T. M. P. Tait and C. E. M. Wagner, Phys. Rev. D **67**, 096006 (2003) [arXiv:hep-ph/0212307].

[11] For a review and original references, see R.N. Mohapatra, *Unification and Supersymmetry*, Springer, New York, (1986).

[12] H. Georgi, A. K. Grant and G. Hailu, Phys. Lett. B **506**, 207 (2001) [arXiv:hep-ph/0012379].

[13] H. Davoudiasl, J. L. Hewett and T. G. Rizzo, Phys. Rev. D **63**, 075004 (2001) [arXiv:hep-ph/0006041].

[14] T. Gherghetta and A. Pomarol, Nucl. Phys. B **586**, 141 (2000) [arXiv:hep-ph/0003129].

[15] See, for example, Ref. 2 and references therein.

[16] M. E. Peskin and T. Takeuchi, Phys. Rev. D **46**, 381 (1992).

[17] T. G. Rizzo, Phys. Rev. D **50**, 2256 (1994) [arXiv:hep-ph/9403241]; G. Altarelli, R. Casalbuoni, S. De Curtis, N. Di Bartolomeo, R. Gatto and F. Feruglio, Phys. Lett. B **318**, 139 (1993).

[18] C. P. Burgess, S. Godfrey, H. Konig, D. London and I. Maksymyk, Phys. Lett. B **326**, 276 (1994) [arXiv:hep-ph/9307337]; I. Maksymyk, C. P. Burgess and D. London, Phys. Rev. D **50**, 529 (1994) [arXiv:hep-ph/9306267].

[19] J. Erler, "Constraining electroweak physics," arXiv:hep-ph/0310202.

[20] M. A. Luty and R. Sundrum, Phys. Rev. Lett. **70**, 529 (1993) [arXiv:hep-ph/9209255].

[21] R. Barbieri, A. Pomarol and R. Rattazzi, "Weakly coupled Higgsless theories and precision electroweak tests," arXiv:hep-ph/0310285.

[22] B. W. Lee, C. Quigg and H. B. Thacker, Phys. Rev. D **16**, 1519 (1977).

[23] M. J. Duncan, G. L. Kane and W. W. Repko, Nucl. Phys. B **272**, 517 (1986).

[24] F. Gianotti *et al.*, "Physics potential and experimental challenges of the LHC luminosity upgrade," arXiv:hep-ph/0204087.

[25] T. G. Rizzo and J. D. Wells, Phys. Rev. D **61**, 016007 (2000) [arXiv:hep-ph/9906234]; J. Hewett and M. Spiropulu, Ann. Rev. Nucl. Part. Sci. **52**, 397 (2002) [arXiv:hep-ph/0205106].

[26] T. G. Rizzo, JHEP **0306**, 021 (2003) [arXiv:hep-ph/0305077]; T. G. Rizzo, in *Proc. of the APS/DPF/DPB Summer Study on the Future of Particle Physics (Snowmass 2001)* ed. N. Graf, eConf **C010630**, P304 (2001) [arXiv:hep-ph/0109179].

[27] G. Azuelos *et al.*, arXiv:hep-ph/0204031;

[28] T. G. Rizzo, Phys. Rev. D **55**, 5483 (1997) [arXiv:hep-ph/9612304]; J. A. Aguilar-Saavedra *et al.* [ECFA/DESY LC Physics Working Group Collaboration], "TESLA Technical Design Report Part III: Physics at an e+e- Linear Collider," arXiv:hep-ph/0106315.

[29] G. F. Giudice, R. Rattazzi and J. D. Wells, Nucl. Phys. B **544**, 3 (1999) [arXiv:hep-ph/9811291]. See also, E. A. Mirabelli, M. Perelstein and M. E. Peskin, Phys. Rev. Lett. **82**, 2236 (1999) [arXiv:hep-ph/9811337].